

# Improving the Predictive Power of Calculations for the Warm Dense Matter Region

Ann E. Mattsson

Computational Shock and Multiphysics  
Sandia National Laboratories  
Albuquerque, NM 87185

Collaborators:

Dirac Equation: John Wills (LANL) and Torey Semi (CSM).

Functionals: Rickard Armiento (MIT) and Feng Hao (formerly SNL).

Van der Waals': Ryan Wixom (SNL) and George Cragg (SNL)

E-mail: [aematts@sandia.gov](mailto:aematts@sandia.gov)

Web: <http://www.cs.sandia.gov/~aematts/>  
<http://dft.sandia.gov>

IPAM, University of California, Los Angeles, CA, 24 May 2012

**SAND 2012-4211C**



Sandia National Laboratories is a multi program laboratory managed and operated by Sandia Corporation, a wholly owned subsidiary of Lockheed Martin Corporation, for the U.S. Department of Energy's National Nuclear Security Administration under contract DE-AC04-94AL85000.



# Quantum Mechanics

Dirac (1929)

“ The general theory of quantum mechanics is now almost complete... The underlying physical laws necessary for the mathematical theory of a large part of physics and the whole of chemistry are thus completely known, and the difficulty is only that the exact application of these laws leads to equations much too complicated to be soluble. ”

P.A.M. Dirac, Proc. R. Soc. London Ser. A 123, 714 (1929).

# How do we learn from the Quantum Mechanical equations?

Exact Hamiltonian with exact solution.

Exact Hamiltonian with approximate solution.

Approximate Hamiltonians with exact solutions.

Approximate Hamiltonians with approximate solutions.

Ideally we would like to solve for example the non-relativistic limit of the Dirac Equation, the Schrödinger Equation, exactly. Only feasible for one-electron systems such as the Hydrogen atom. Already for the two-electron system of the He atom we need to start doing (at least numerical) approximations. For Condensed Matter systems we cannot expect to solve the SE directly, even with the largest and fastest computers in the world.

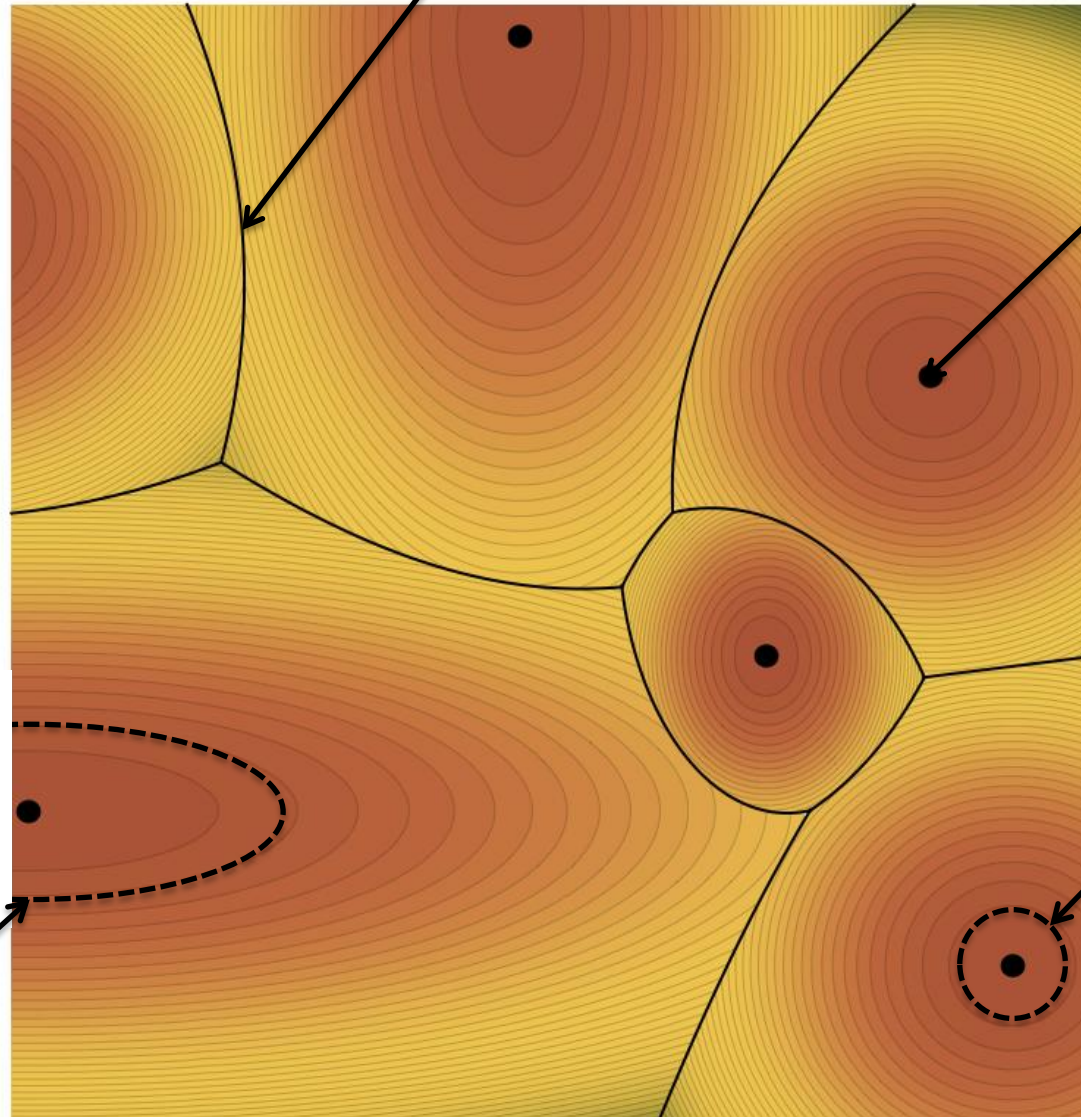


# My personal view of the field

Ann E Mattsson

But using different theories for different types of systems is not truly predictive and also is not helping us to calculate properties at a macroscopic/ engineering scale.

Quasi Particle Theory can take small influences from other types of physics into account.



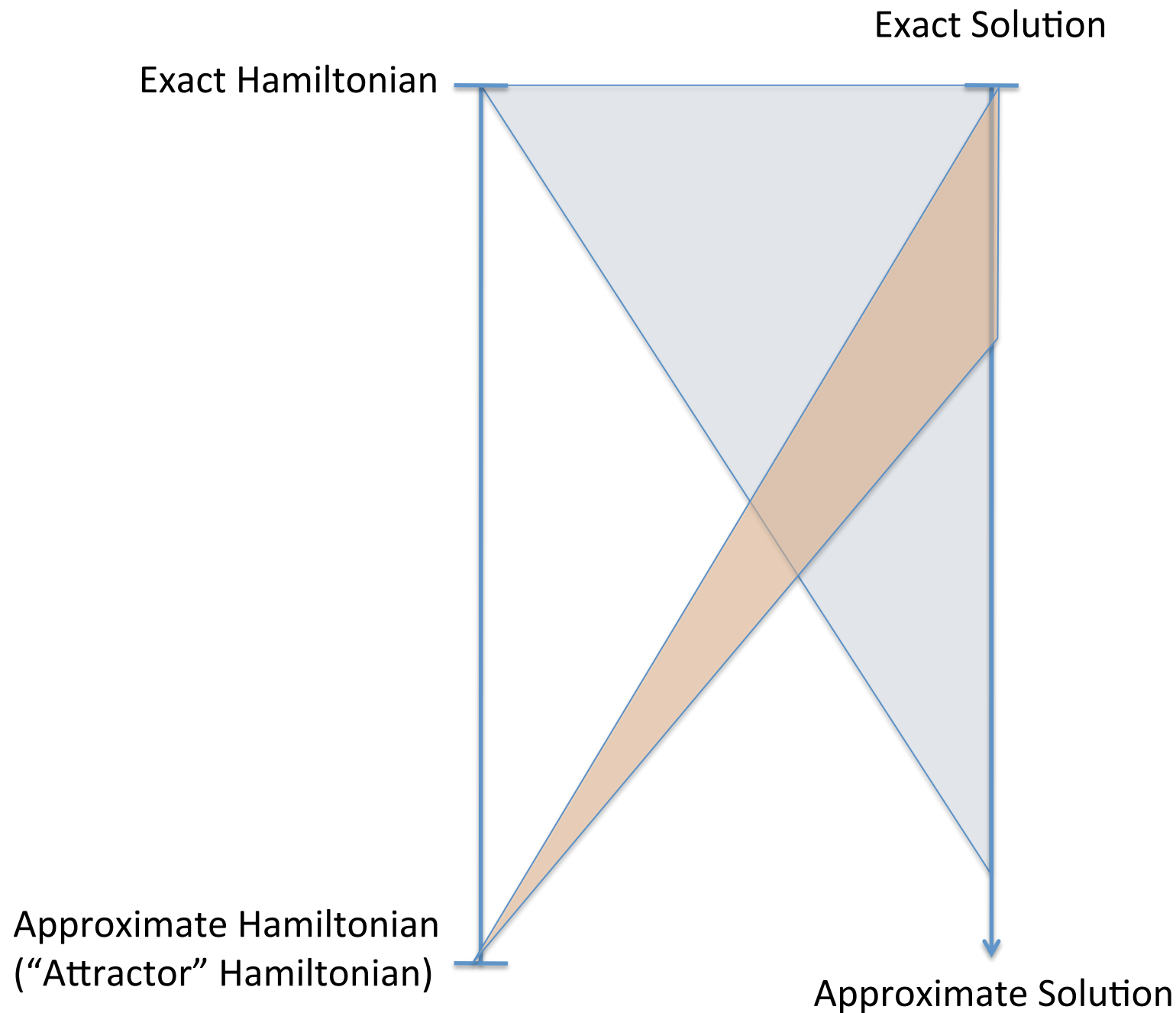
Marginal Physics is quite exciting.

“Attractor” Physics: The dominant physical behavior in a specific type of systems

Perturbation Theory can take small influences from other types of physics into account.



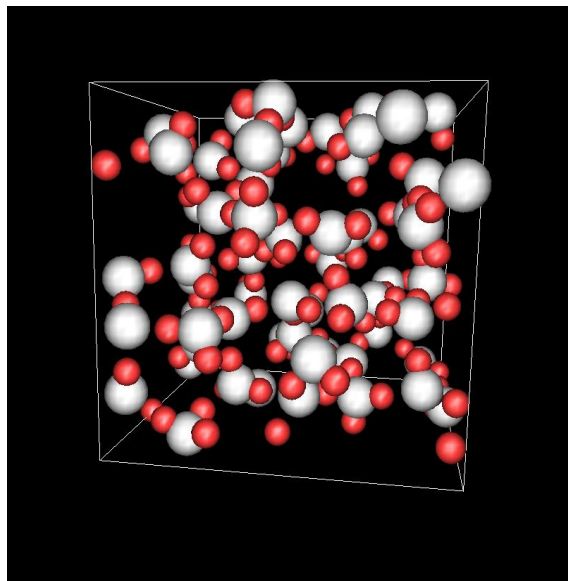
# How do we learn from the Quantum Mechanical equations?



# Speed is also very important

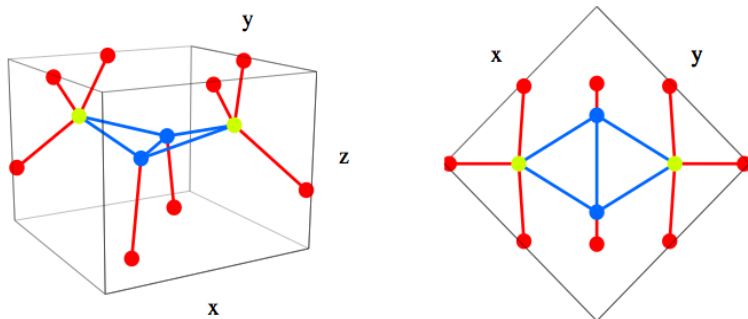
## DFT-MD (also called QMD)

Snap shot of water simulation  
(64 molecules) done with  
AM05. Thomas Mattsson.



DFT is increasingly employed in quantum MD simulations of hundreds of atoms for tens of ps. This application demands functionals that are both accurate and fast. Every calculation with a temperature needs to be done with MD. Examples: Critical points and melting curves for EOS construction; Realistic calculations with water present.

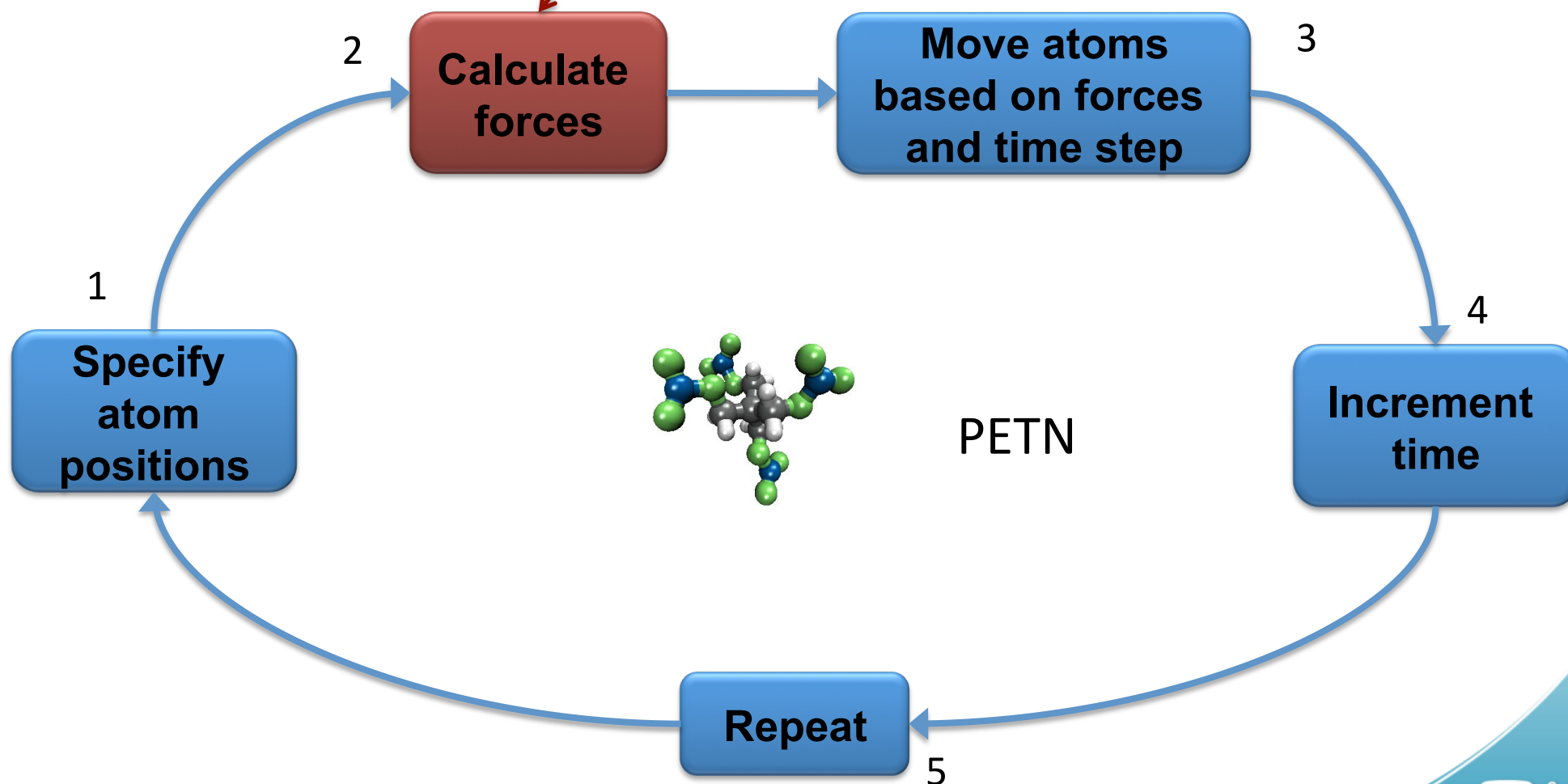
**Large cells and diffusion:** Since all solid state DFT calculations uses periodic boundary conditions, large supercells are required for defect simulations in order to avoid uncontrolled interactions between defects. Calculating diffusion coefficients also require nudge elastic band type calculations where several copies of the same systems are needed.



The Si  $\langle 110 \rangle$  - split interstitial

# Molecular Dynamics

DFT-MD (or a AIMD or QMD): Forces calculated with DFT.  
Classical MD: Forces calculated with force fields or potentials.



Adapted from slides by Ryan Wixom, SNL.



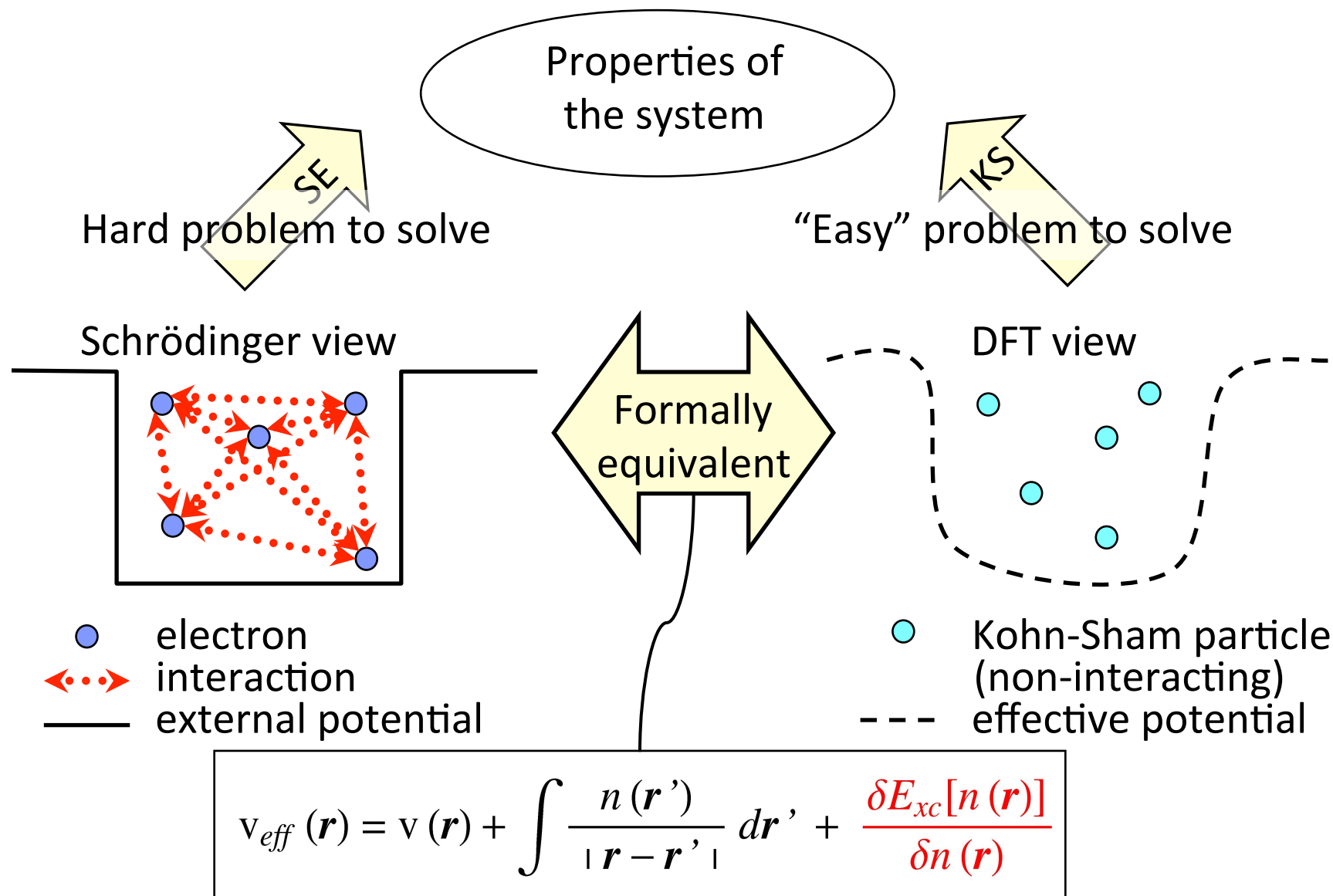
# Walter Kohn awarded the Nobel Prize in Chemistry 1998 for Density Functional Theory



Hohenberg-Kohn theorem:  
Phys. Rev. **136**, B864 (1964).  
The **electron density** contains all  
information needed to determine  
ground state properties of a system.

Kohn-Sham equations:  
Phys. Rev. **140**, 1133 (1965).  
Practical scheme for solving the  
quantum mechanical problem based  
on the HK theorem.

# DFT versus the Schrödinger Equation



All many-body effects are included in the effective potential via the

Exchange-Correlation functional,  $E_{xc}[n(\mathbf{r})]$ .

# Kohn-Sham equations:

$$\left( -\frac{\hbar^2}{2m} \nabla^2 + v_{eff}(\mathbf{r}) \right) \psi_\nu(\mathbf{r}) = \epsilon_\nu \psi_\nu(\mathbf{r}) \quad \nu = 1, 2, \dots, N$$

$$n(\mathbf{r}) = \sum_{\nu=1}^N |\psi_\nu(\mathbf{r})|^2$$

$$v_{eff}(\mathbf{r}) = v(\mathbf{r}) + \int \frac{n(\mathbf{r}')}{|\mathbf{r} - \mathbf{r}'|} d\mathbf{r}' + \frac{\delta E_{xc}[n(\mathbf{r})]}{\delta n(\mathbf{r})}$$

If we had the **divine exchange-correlation functional**, these equations would give exactly the same density as the Schrödinger Equation, and thus via the HK theorem, we should be able to extract all information about the system.



# Approximations for the exchange-correlation functional

$$\left( -\frac{\hbar^2}{2m} \nabla^2 + v_{eff}(\mathbf{r}) \right) \psi_\nu(\mathbf{r}) = \epsilon_\nu \psi_\nu(\mathbf{r}) \quad \nu = 1, 2, \dots, N$$

$$n(\mathbf{r}) = \sum_{\nu=1}^N |\psi_\nu(\mathbf{r})|^2$$

$$v_{eff}(\mathbf{r}) = v(\mathbf{r}) + \int \frac{n(\mathbf{r}')}{|\mathbf{r} - \mathbf{r}'|} d\mathbf{r}' + \frac{\delta E_{xc}[n(\mathbf{r})]}{\delta n(\mathbf{r})}$$

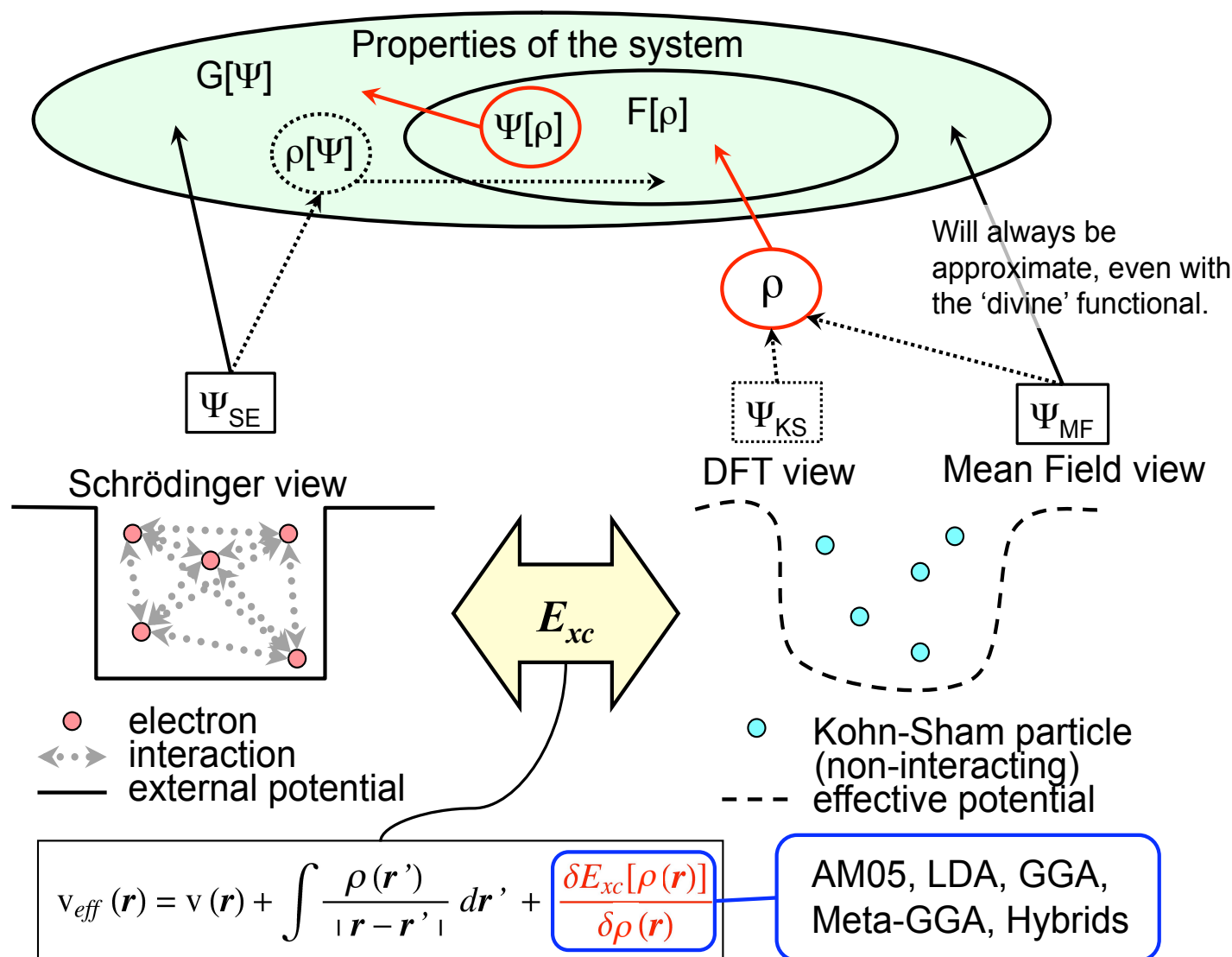
AM05, LDA,  
GGA, Meta-  
GGA, Hybrids

The form of the divine exchange-correlation functional is unknown.  
We need to find good approximations.  
There is nothing like a free lunch.

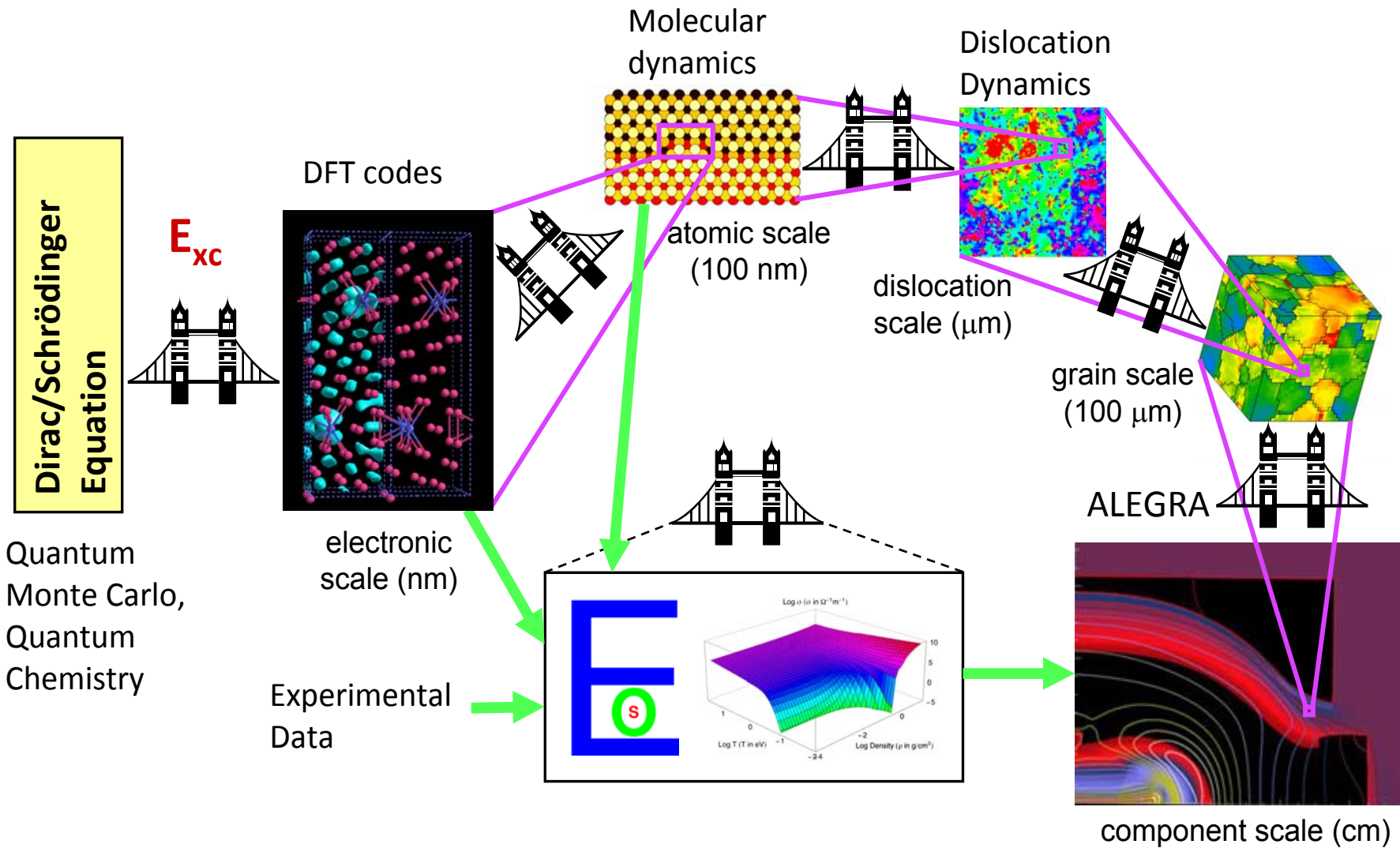
# DFT versus Mean Field Theory

From "Metallic Systems: A Quantum Chemist's Perspective", the chapter "Some practical considerations for density functional theory studies of chemistry at metal surfaces" published by Taylor and Francis in 2011.

Density =  $\rho$  in chemistry  
 $n$  in physics



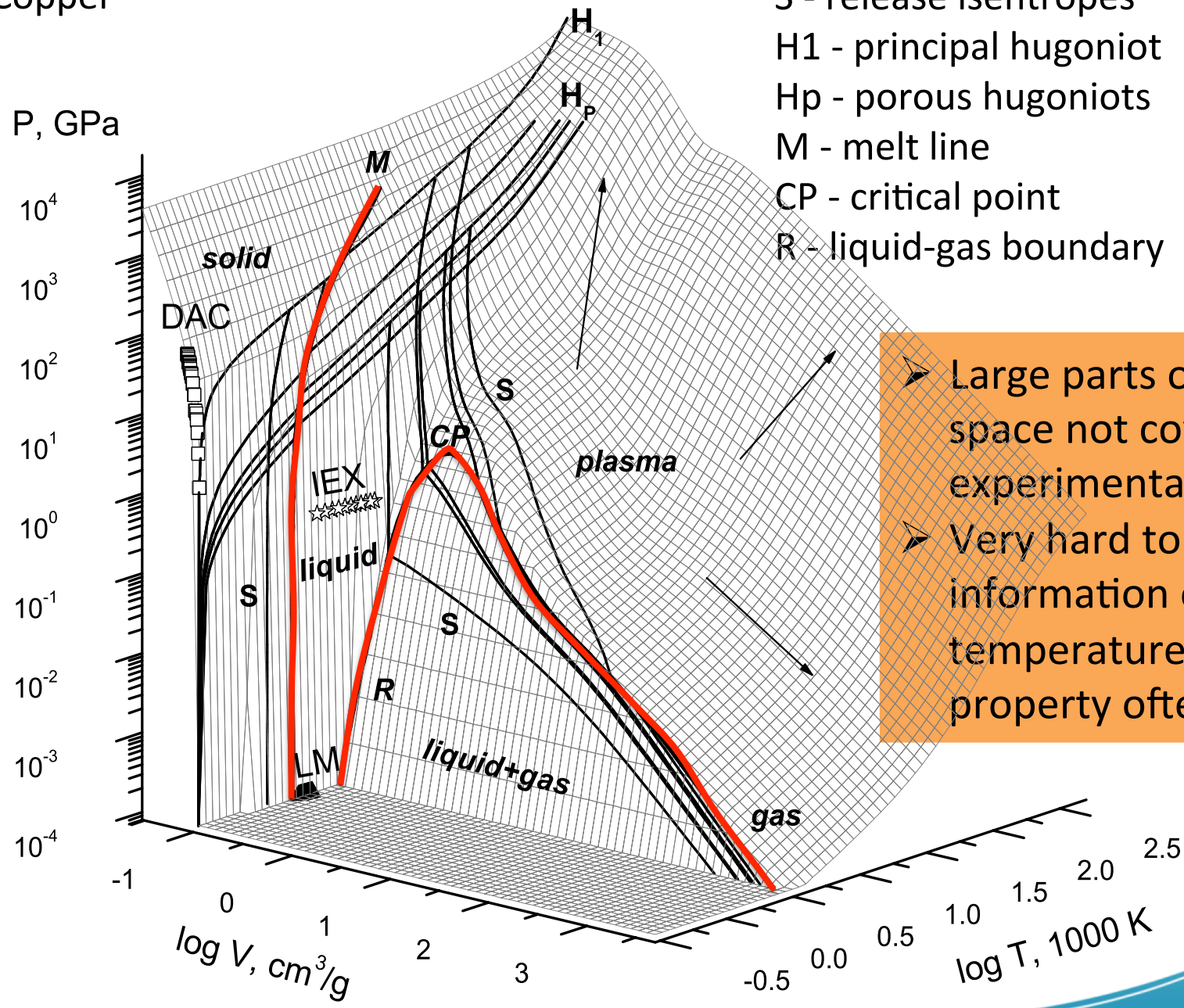
# Bridges between Fundamental Law of Nature and Engineering





# Equation of State: Example of Material input

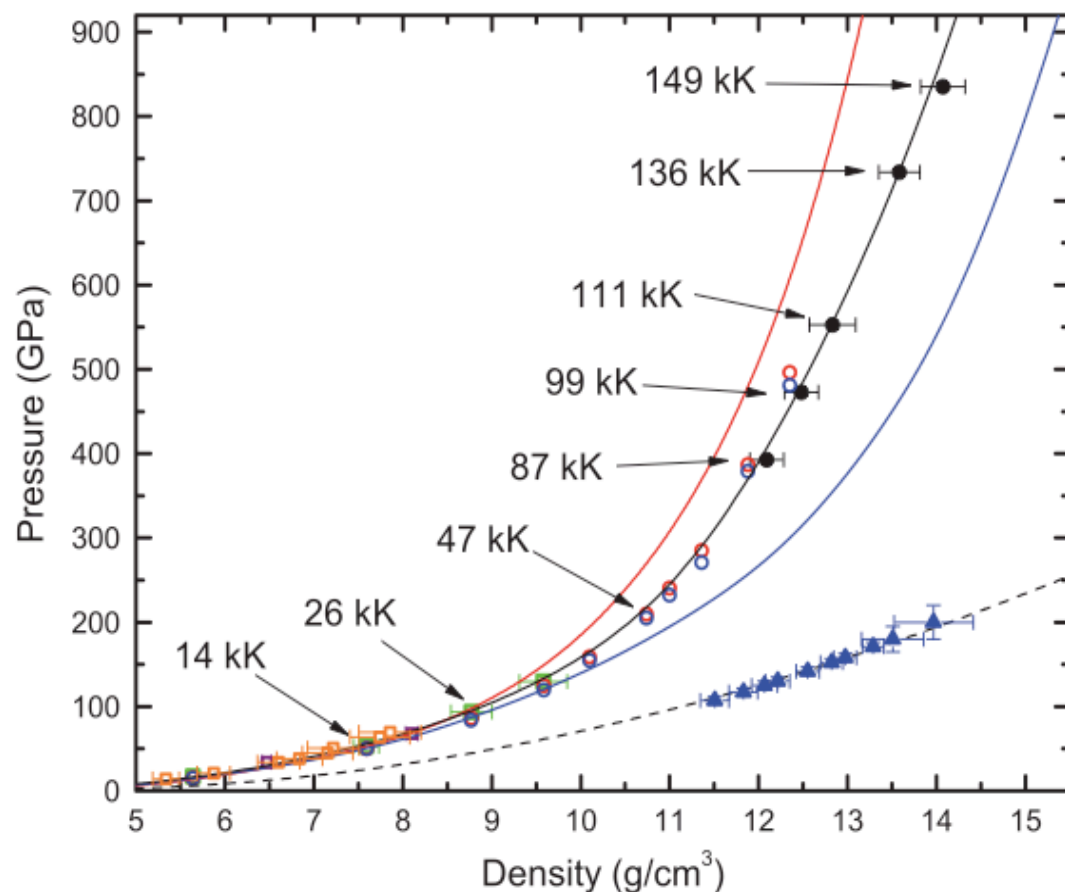
Copper



DAC - diamond anvil cell measurements  
IEX - isobaric expansion experiments  
S - release isentropes  
H<sub>1</sub> - principal hugoniot  
H<sub>p</sub> - porous hugoniot  
M - melt line  
CP - critical point  
R - liquid-gas boundary

- Large parts of parameter space not covered by any experimental technique.
- Very hard to get information on temperature, this property often inferred.

# Predictive DFT calculations for EOS construction: Example of Xe



Seth et al. PRL 105, 085501 (2010)

Red circle: LDA

Blue circle: AM05

Black circles: Z data

Black line: New EOS 5191

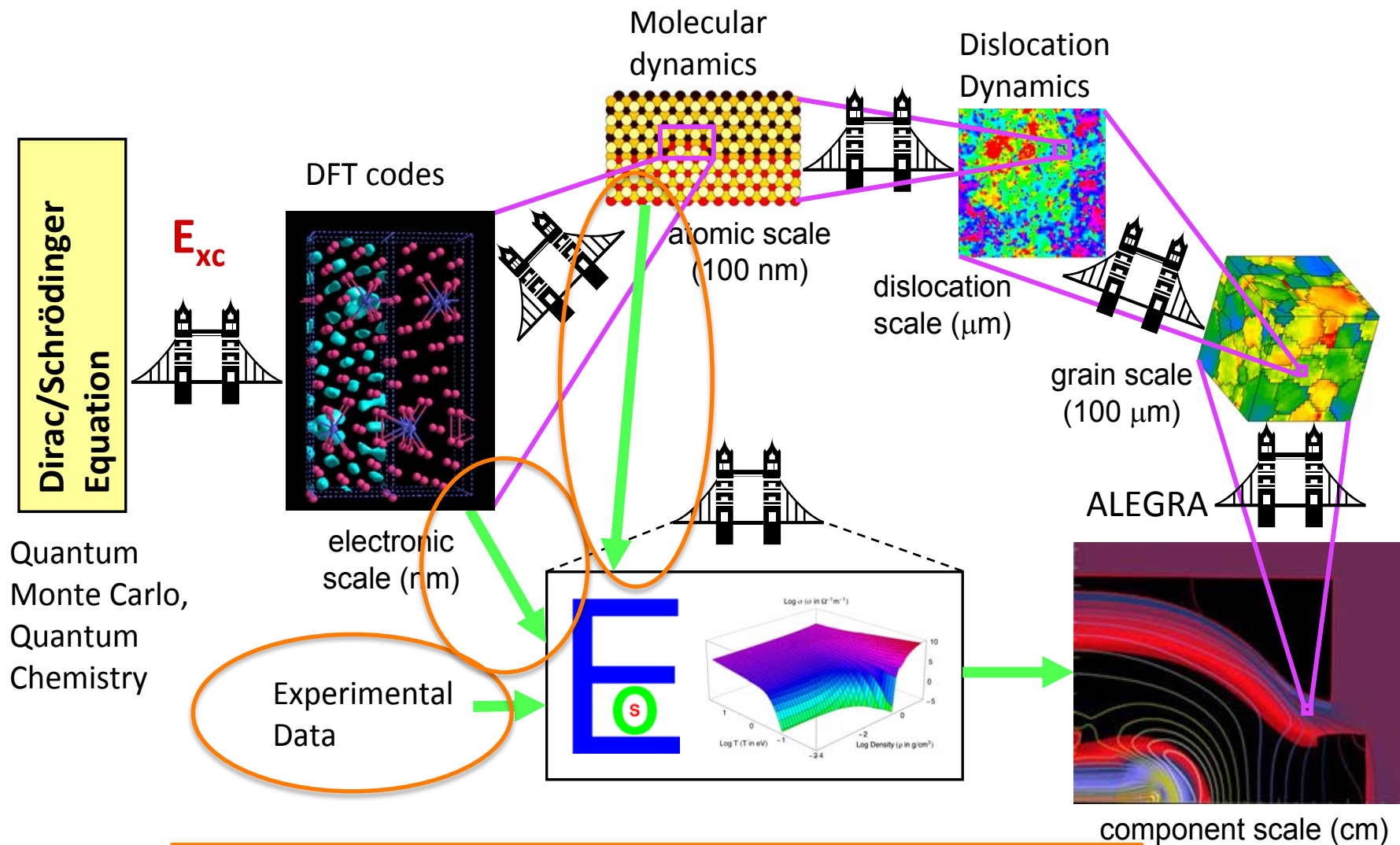
Blue line: SESAME 5190

Red line: LEOS 540

Note: DFT calculations published *before* Z data was available. Shown is the Hugoniot. DFT data is added also in other parts of phase space (e.g., cold curve and melt line).

FIG. 3 (color).  $P$ - $\rho$  Hugoniot plot. Lines and symbols as in Fig. 2. Black dashed line, 5191 298 K isotherm; blue triangles, solid xenon compression data [17]. Also indicated are Hugoniot temperatures calculated using 5191. Our DFT calculated isotherm [37] agrees with the experimental data [17].

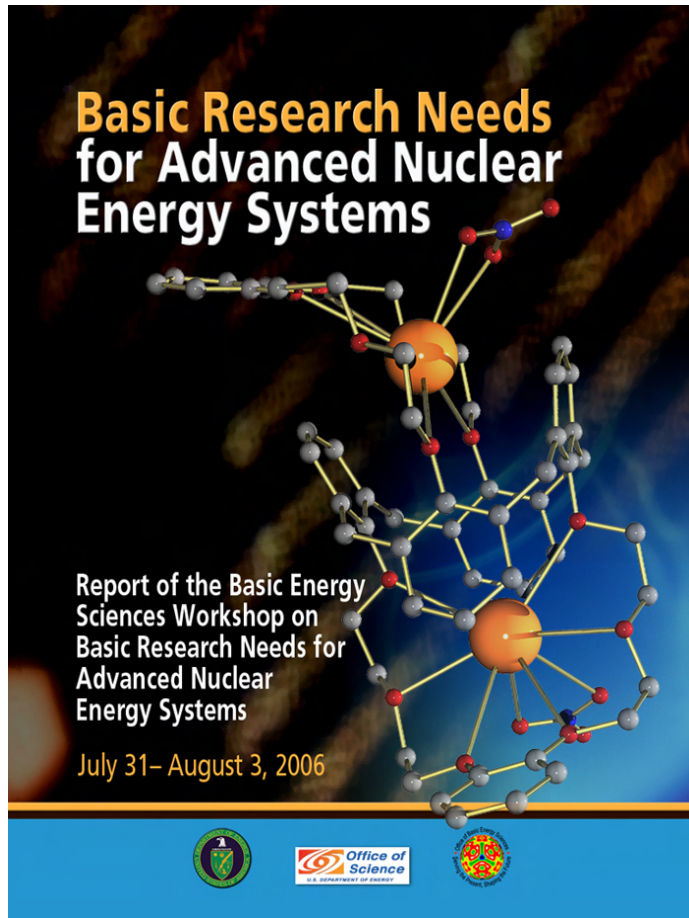
# Bridges between Fundamental Law of Nature and Engineering



The ability to perform high-fidelity calculations is most important for cases where experiments are impossible, dangerous, and/or prohibitively expensive to perform.



# Better ab initio methods for f-electron systems identified as a Basic Research Need



Scientific grand challenges:

- Resolving the f-electron challenge to master the chemistry and physics of actinides and actinide-bearing materials.
- Developing a first-principles, multiscale description of materials properties in complex materials under extreme conditions.
- Understanding and designing new molecular systems to gain unprecedented control of chemical selectivity during processing.

# We want to be able to do DFT based calculations for all materials

While DFT is very successful for many materials and many properties, not all materials and properties are equally well treated with DFT. This is the case with, for example, actinides.

We have two problems:

- High atomic numbers means relativistic effects.
- Localized  $f$ -electrons means DFT exchange-correlation functionals (including AM05) are not accurate enough.

# Dirac, Scalar Relativistic, and Spin Orbit

Incorporating Relativity:  
 Scalar Relativistic (**SR**), SR+perturbative spin-orbit (**SO**), and **Dirac**

Basis functions for “FP-” methods (“-LMTO”, “LAPW”) are solutions to an *underlying equation* (SR or Dirac) for a muffin-tin potential<sup>(\*)</sup>; *i.e.*, they are *spherical- or plane-waves augmented* by “exact” solutions to the (atomic-like) potential within the muffin-tin spheres.

Underlying equation:

In all electron codes, relativity is generally dealt with in one of three ways:

- bases ( $\psi$ ) generated using the **Dirac equation**:

$$(\mathcal{H}_D + V - mc^2) \psi = e\psi, \quad \mathcal{H}_D = c\alpha \cdot p + \beta mc^2 \quad \boxed{\text{Dirac}}$$

The Dirac equation can be written in terms of the Koelling-Harmon equation:

$$(\mathcal{H}_D + V - e)\psi = (\mathcal{H}_{SR} - e)\psi - V_{SO}(r)\sigma \cdot \mathcal{L} \begin{pmatrix} 1 & 0 \\ 0 & 0 \end{pmatrix} \psi \quad \boxed{\text{K-H}}$$

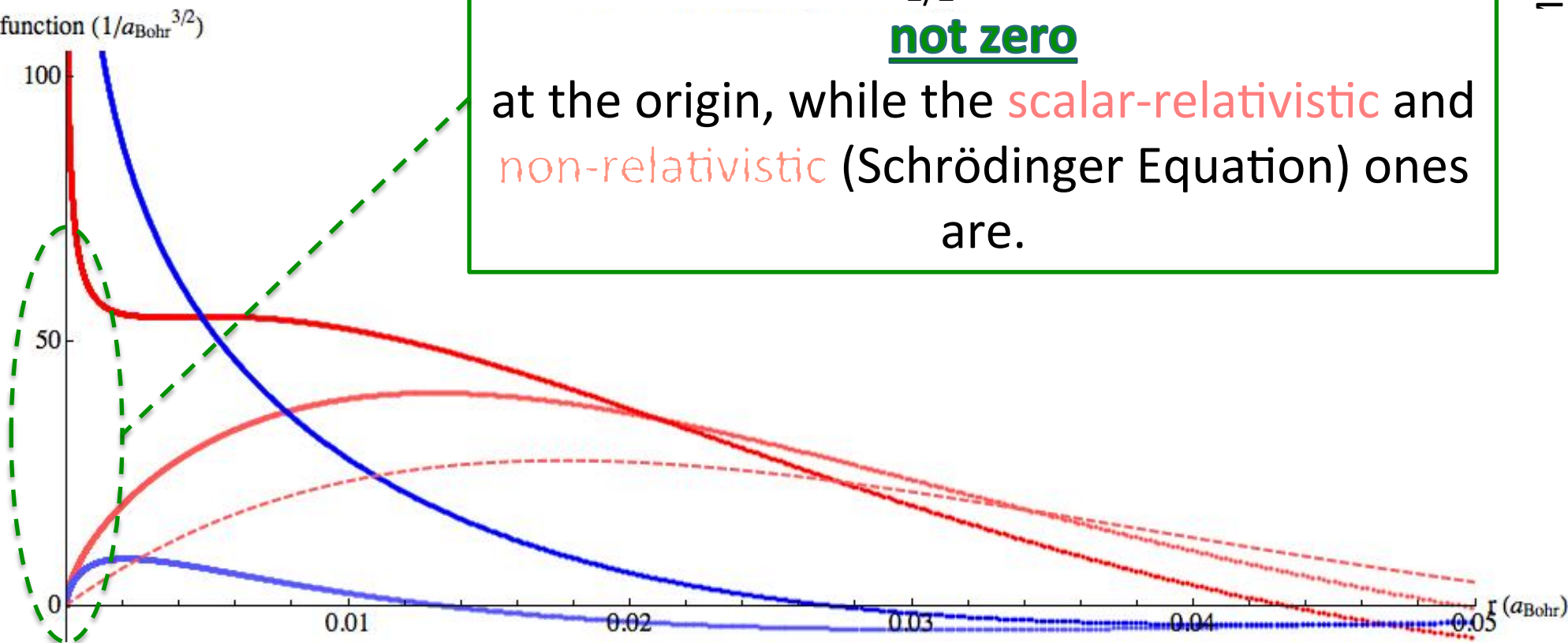
D. D. Koelling and B. N. Harmon, Journal of Physics C: Solid State Physics 10, 3107 (1977)

- The scalar relativistic approximation (**SR**) amounts to setting  $V_{SO} = 0$ .
- SR + perturbative spin orbit (**SO**): using SR bases, solve the full Koelling Harmon equation with  $V_{SO}$  treated variationally.

(\*) atomic-like in spheres surrounding atoms, constant in between

# Heavy Materials: The problematic $p_{1/2}$ states

The **Dirac**  $p_{1/2}$  wavefunction is **not zero** at the origin, while the **scalar-relativistic** and **non-relativistic** (Schrödinger Equation) ones are.



Conclusion: We need to use a DFT method based on the Dirac Equation. This has been implemented into the RSPt code and we are just now testing what this gives as results.



# Relativistic Kohn-Sham equations: Functionals

$$\left( c \boldsymbol{\alpha} \cdot \left( \mathbf{p} + \frac{e \mathbf{A}_{eff}}{c} \right) + \begin{pmatrix} I & 0 \\ 0 & I \end{pmatrix} V_{eff}(\mathbf{r}) + \beta m c^2 \right) \psi_n(\mathbf{r}) = E_n \psi_n(\mathbf{r})$$

$$V_{eff}(\mathbf{r}) = -e \left( A_{ext}^0(\mathbf{r}) + \int d^3 r' \frac{J^0(\mathbf{r}')}{|\mathbf{r} - \mathbf{r}'|} + \frac{\delta E_{xc}[J^\mu]}{\delta J^0(\mathbf{r})} \right)$$

$$e \mathbf{A}_{eff}(\mathbf{r}) = -e \left( \mathbf{A}_{ext}(\mathbf{r}) + \int d^3 r' \frac{\mathbf{J}(\mathbf{r}')}{|\mathbf{r} - \mathbf{r}'|} + \frac{\delta E_{xc}[J^\mu]}{\delta \mathbf{J}(\mathbf{r})} \right)$$

$$J^\mu = (J^0, \mathbf{J}) = -e \sum_{-mc^2 < E_n < E_F} (\psi_n^\dagger \psi_n, \psi_n^\dagger \boldsymbol{\alpha} \psi_n)$$

But functionals available from non-relativistic Kohn-Sham theory use spin densities, not currents. The vector potential term is the tricky one, coupling upper and lower components.

# From currents to spin densities

Spin density:

$$\mathbf{S} = - \sum_{-mc^2 < E_n < E_F} \psi_n^\dagger \beta \boldsymbol{\Sigma} \psi_n \quad \Sigma_k = \begin{pmatrix} \sigma_k & 0 \\ 0 & \sigma_k \end{pmatrix}$$

Gordon decomposition

$$\mathbf{J} = \mathbf{I} + \mu_B \nabla \times \mathbf{S}$$

$$\mathbf{I} = \frac{e}{2mc} \sum_{-mc^2 < E_n < E_F} \left\{ \psi_n^\dagger \beta \left[ \left( \mathbf{p} - \frac{e\mathbf{A}_{eff}}{c} \right) \psi_n \right] + \left[ \left( \mathbf{p} - \frac{e\mathbf{A}_{eff}}{c} \right) \psi_n \right]^\dagger \beta \psi_n \right\}$$

Orbital current: Neglecting this gives...

# Approximate Dirac for spin density functionals

$$\left( c \boldsymbol{\alpha} \cdot \mathbf{p} + \mu_B \beta \boldsymbol{\Sigma} \cdot \mathbf{B}_{eff} + \begin{pmatrix} I & 0 \\ 0 & I \end{pmatrix} V_{eff}(\mathbf{r}) + \beta mc^2 \right) \psi_n(\mathbf{r}) = E_n \psi_n(\mathbf{r})$$

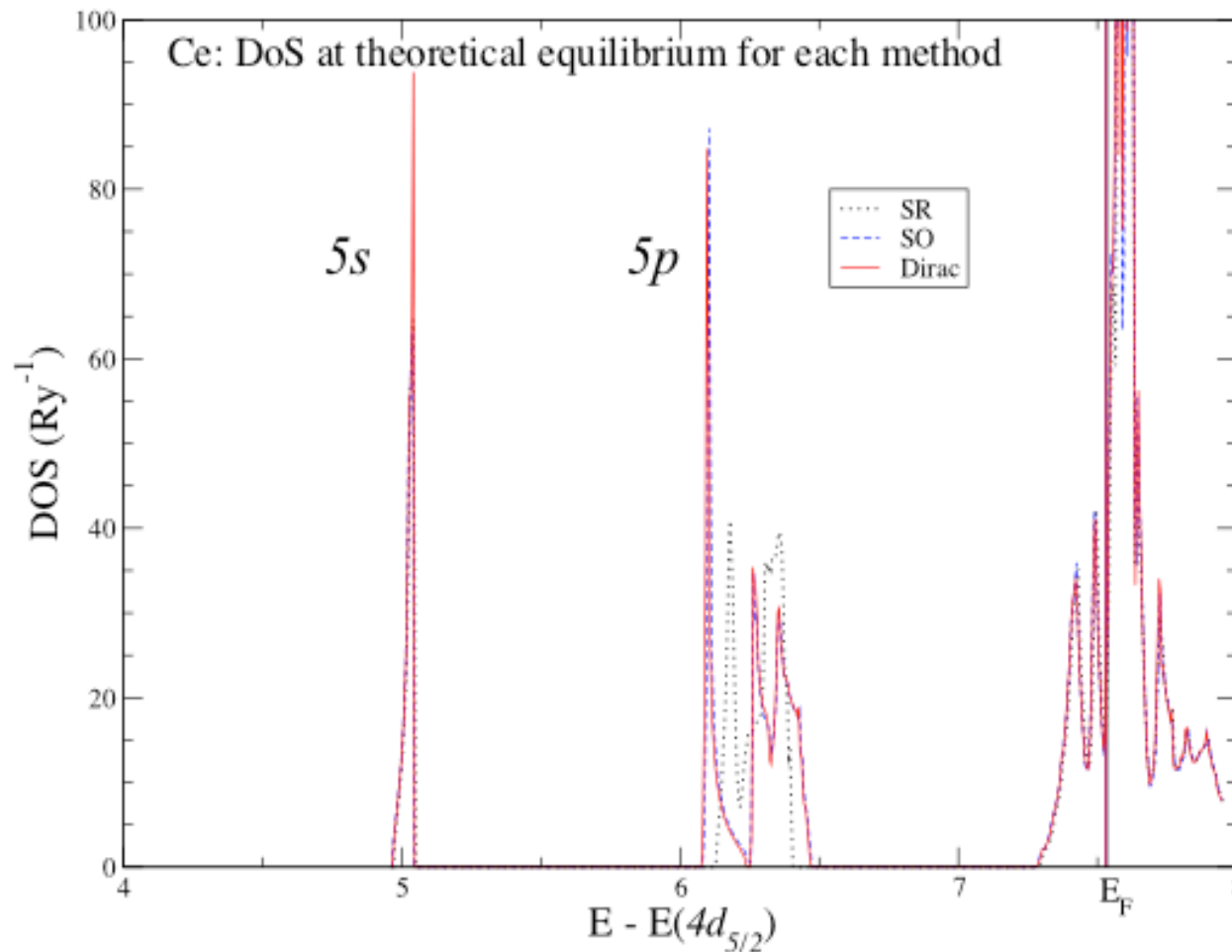
$$V_{eff}(\mathbf{r}) = -e \left( A_{ext}^0(\mathbf{r}) + \int d^3r' \frac{J^0(\mathbf{r}')}{|\mathbf{r} - \mathbf{r}'|} + \frac{\delta E_{xc}[J^\mu]}{\delta J^0(\mathbf{r})} \right)$$

$$\mu_B \mathbf{B}_{eff}(\mathbf{r}) = \left( \mu_B \mathbf{B}_{ext}(\mathbf{r}) + \int d^3r' \frac{\mathbf{M}(\mathbf{r}')}{|\mathbf{r} - \mathbf{r}'|} + \frac{\delta E_{xc}[J^0, \mathbf{M}]}{\delta \mathbf{M}(\mathbf{r})} \right)$$

$$\mathbf{M} = \mu_B \mathbf{S}$$

Now ordinary DFT spin functionals can be used.

# Core and valence electrons



## DoS for Ce

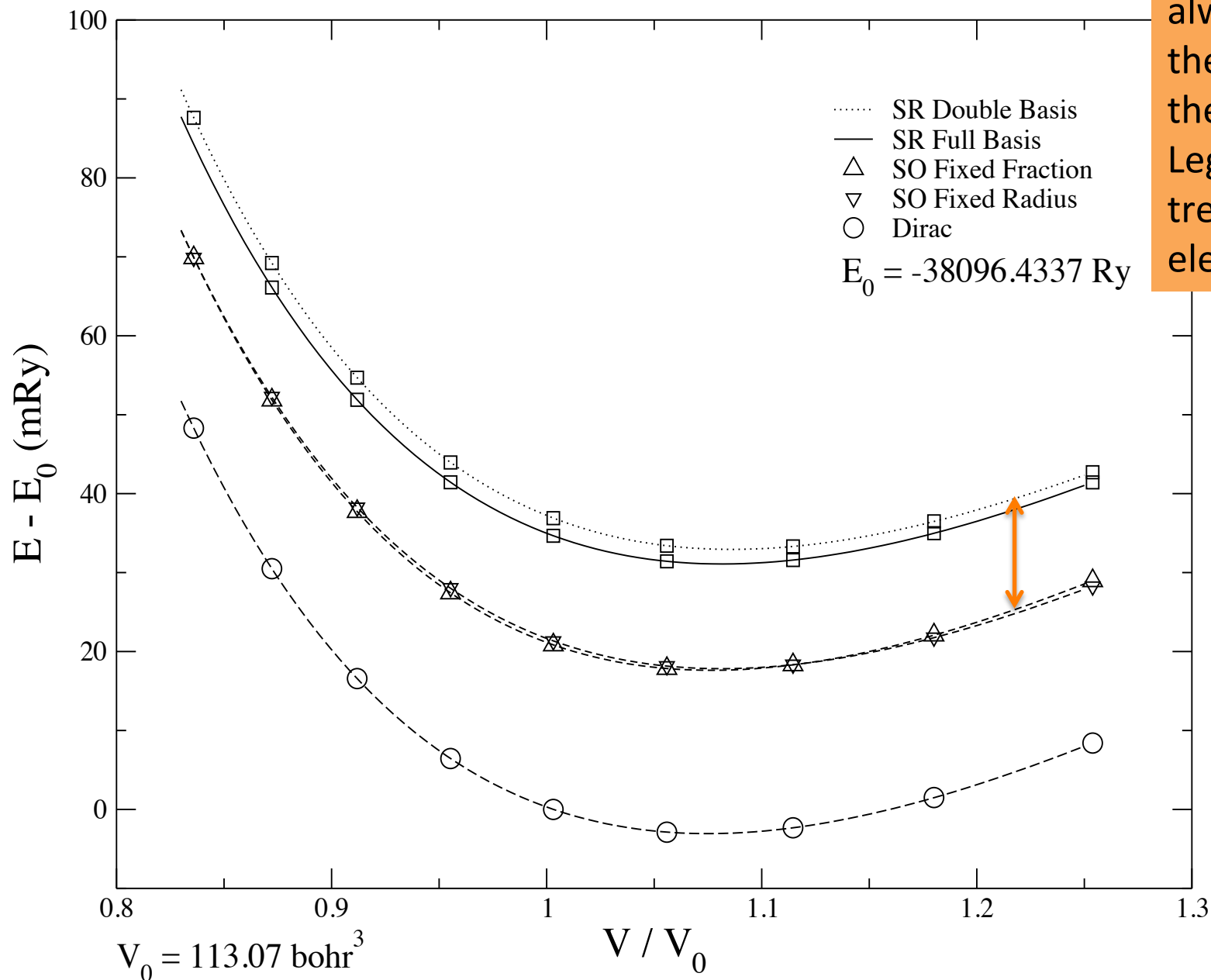
Calculated at theoretical equilibria with AM05 using

- SR (black dotted)
- SO (blue dashed)
- and
- Dirac (red solid)

Energies are relative to the Ce  $4d_{5/2}$  core state which should reasonably be the same in all three calculations.

- Dirac and SO seem to give almost identical DOS, at least for occupied states
- All DOS align except for the SR 5p states; treating these states as SR would seem to be inaccurate.

# Probing different relativistic treatments in Au: Setting the stage



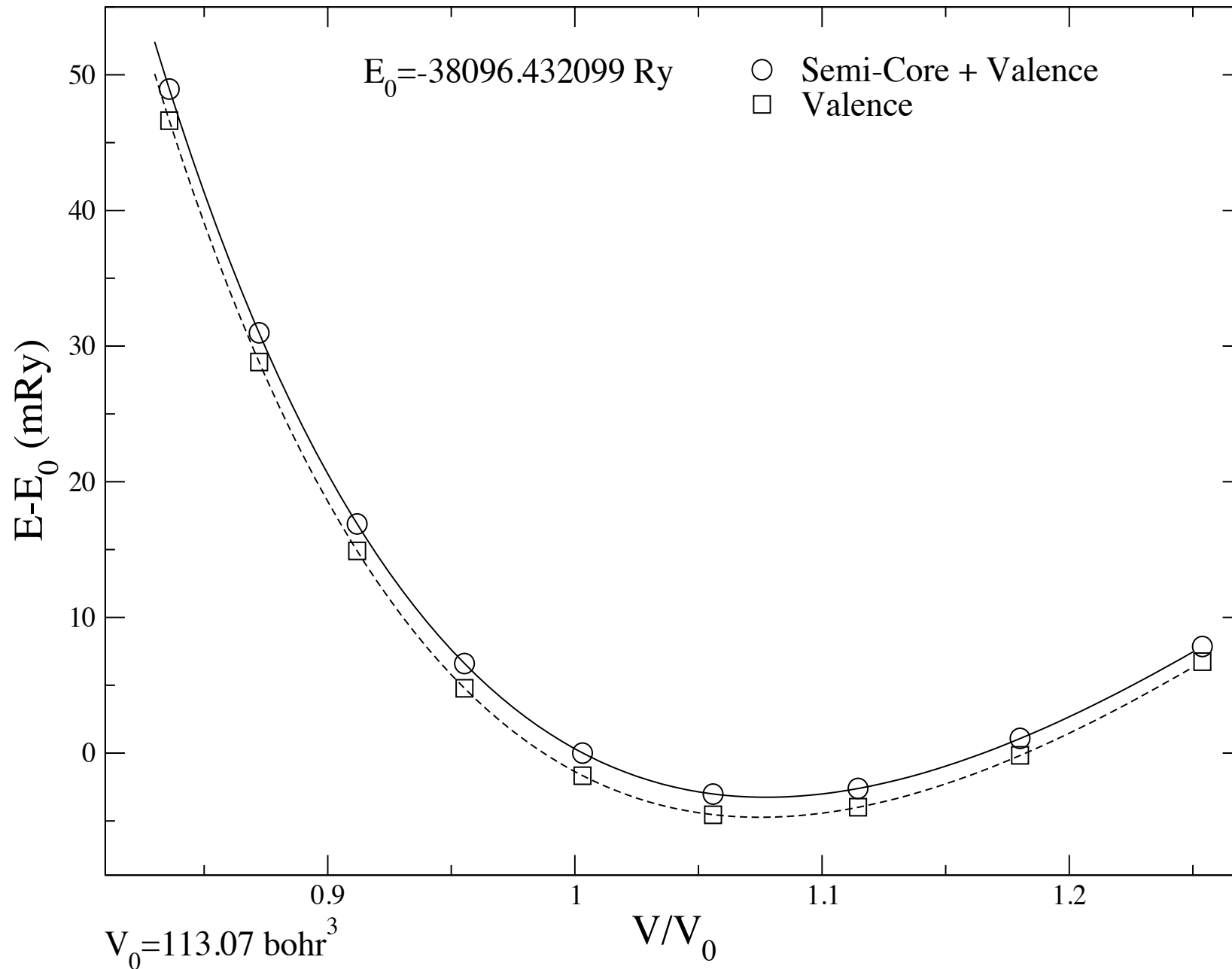
Core electrons are always treated with the Dirac equation in the RSPt code. Legends indicates treatment for valence electrons.

Conclusion: The spin-orbit coupling among the bonding valence electrons (10 5d and 1 6s) is small, but not insignificant.



# All Au electrons treated with the Dirac equation: Semi-Core (5p) and Valence

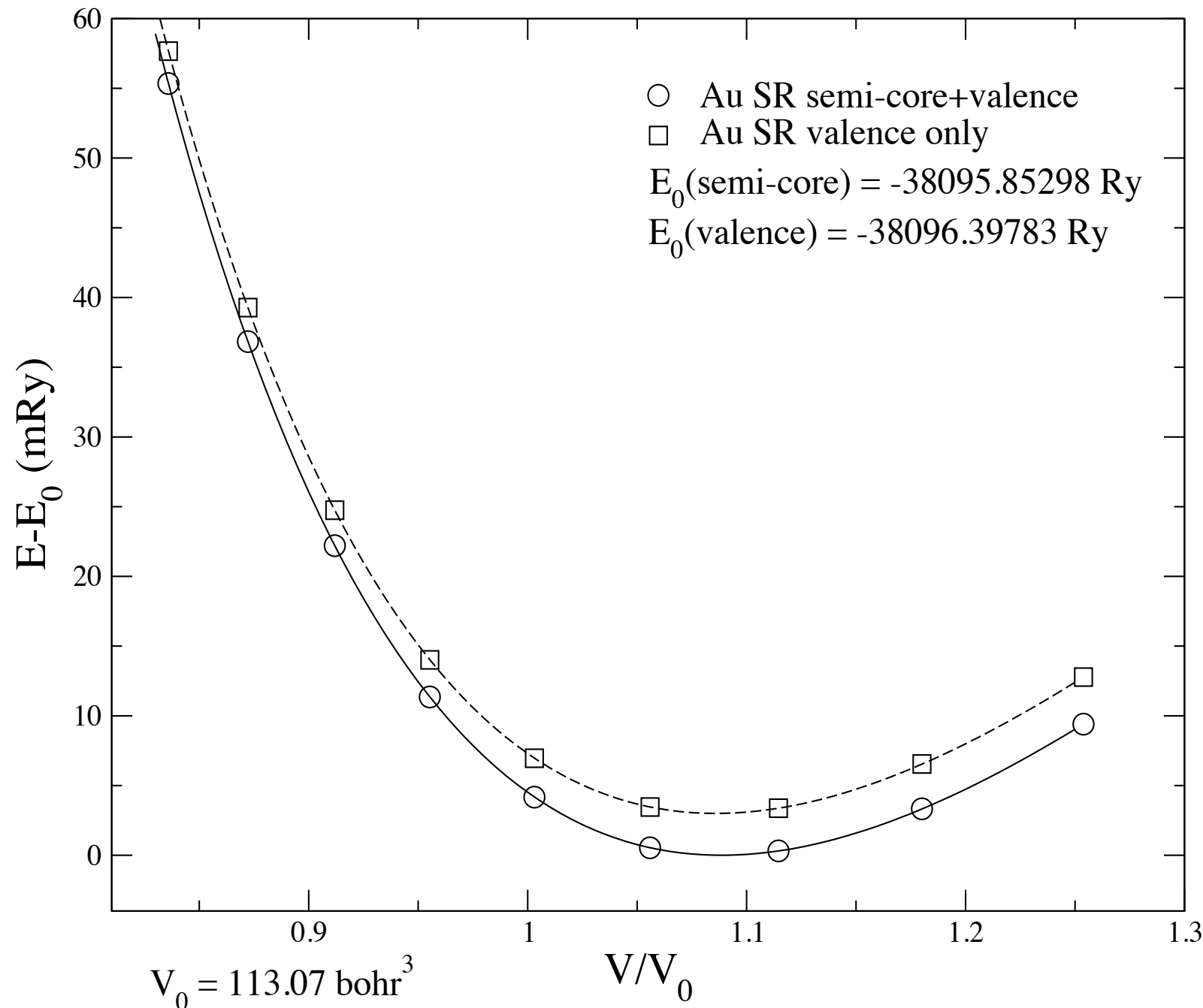
Ann E Mattsson



The 5p electrons are well separated from the rest of the valence and can be treated in the core (with no interaction with the rest of the valence).

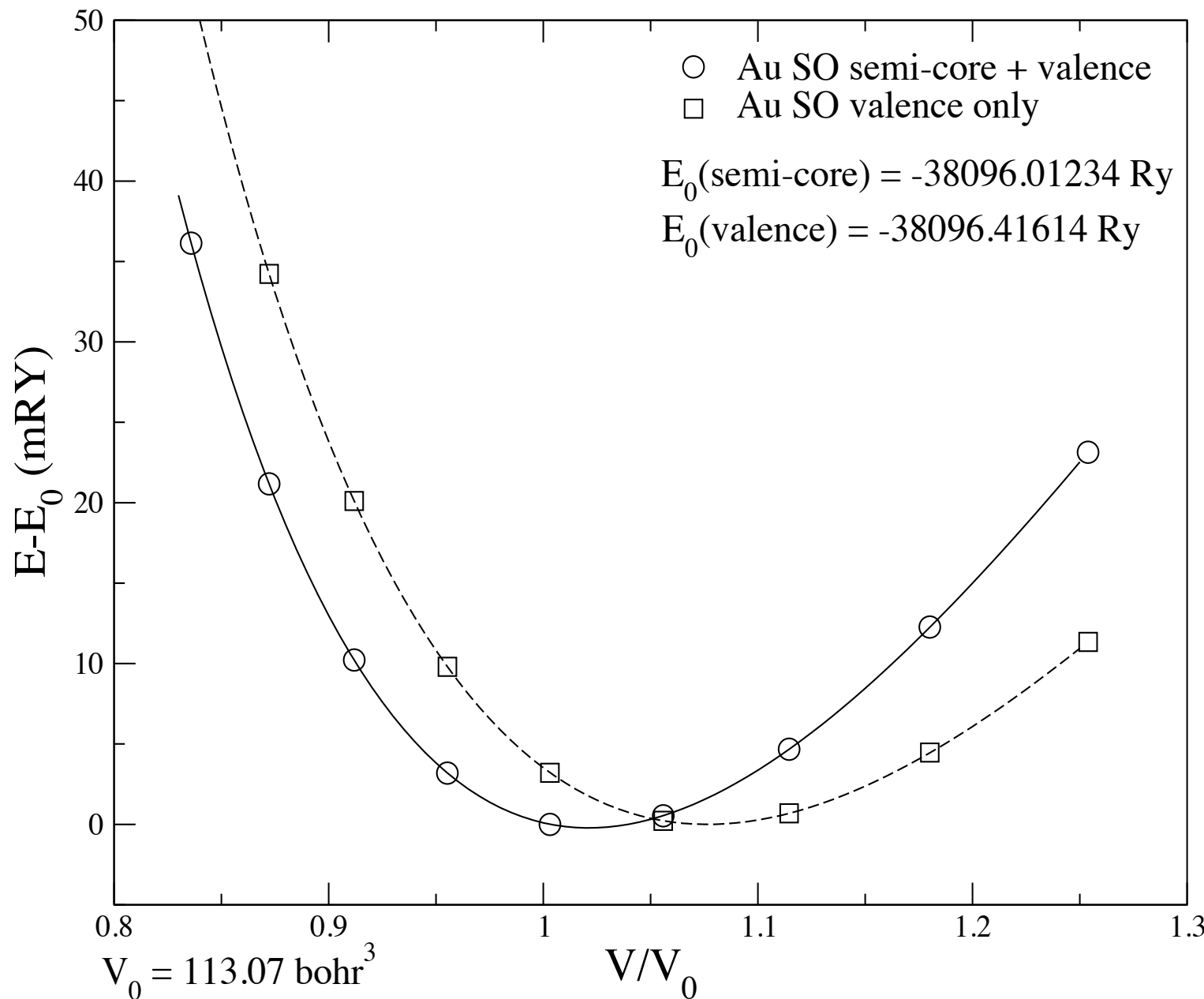
# Au 5p treated with Dirac vs Scalar relativistic

Ann E Mattsson



Since the non-bonding 5p semi-core electrons do not participate in the binding as the rest of the valence, treating them scalar relativistically gives the same error for all volumes.

# Au 5p: Dirac vs variational spin-orbit coupling

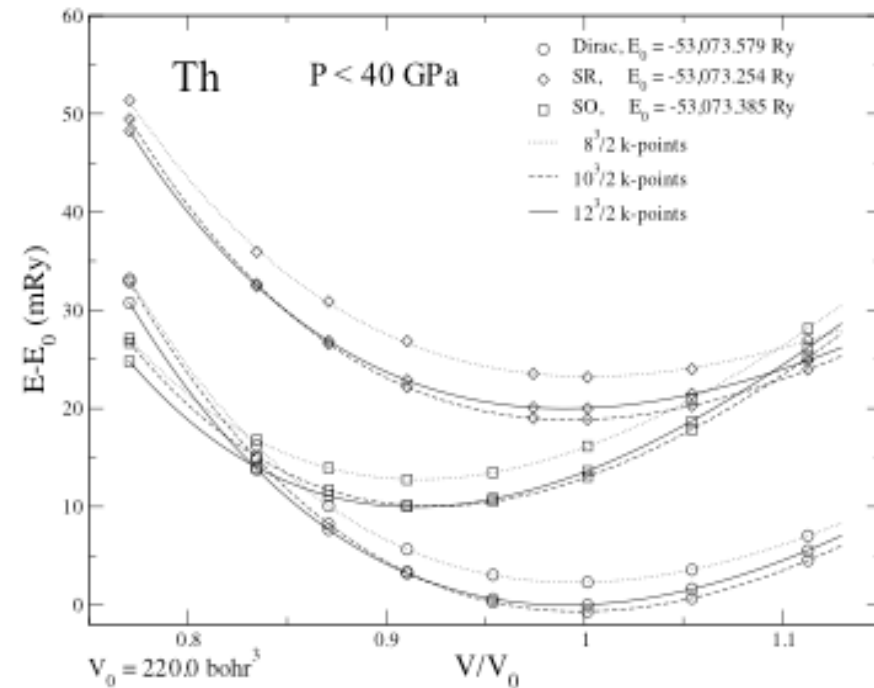
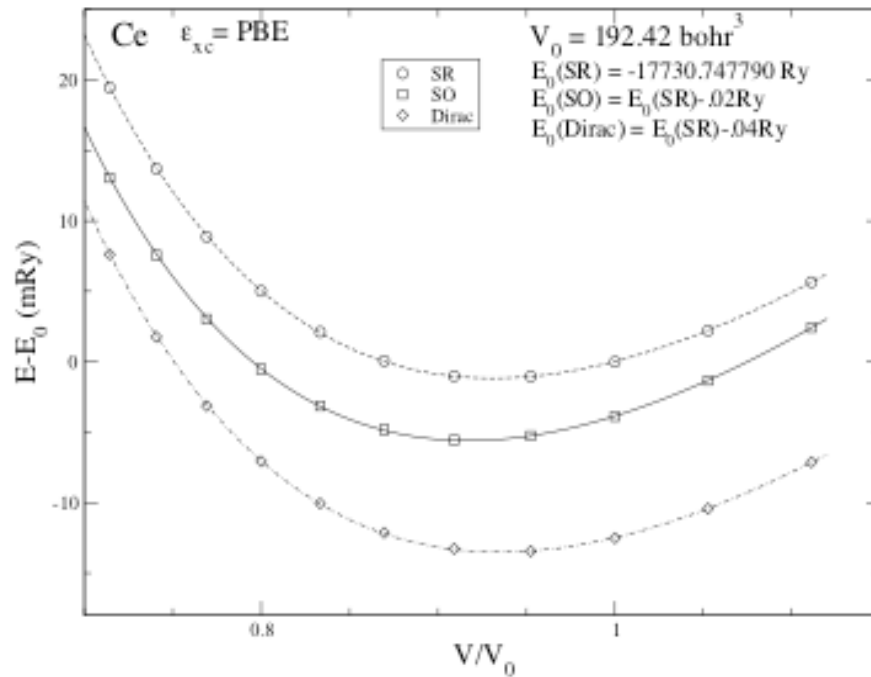


Variationally adding a relativistic treatment (spin-orbit coupling) to the 5p electrons does not mimic the full Dirac treatment.

The spin-orbit coupling among the 5p electrons is strong, not a small perturbation, and the erroneous behavior of the unperturbed basis at the nuclei results in an invalid treatment.

# Ce vs Th

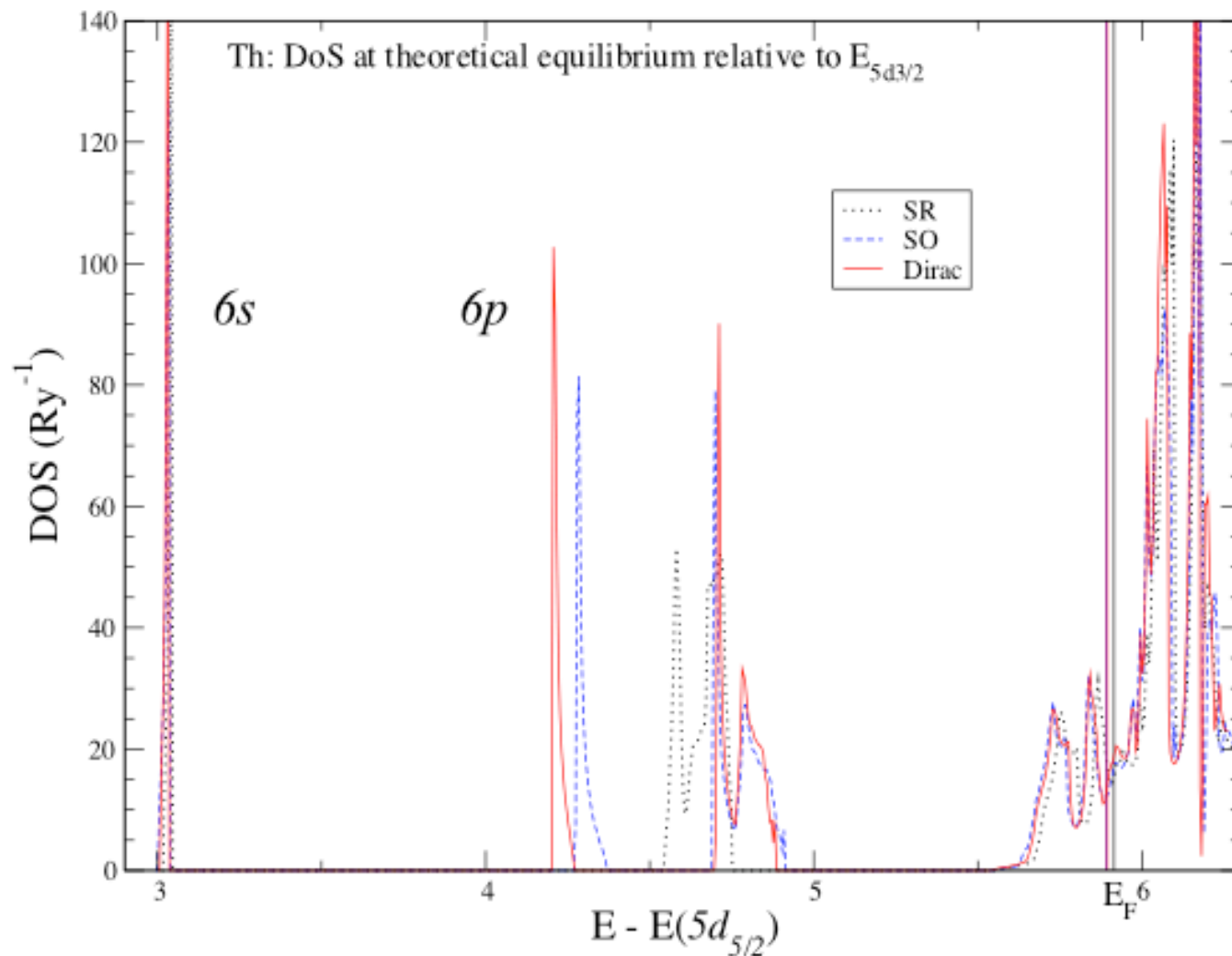
*fcc* Ce and *fcc* Th with PBE  $\epsilon_{xc}$  and SR, SO, and Dirac methods



## Compare Ce and Th

- Similar behavior, much more striking in Th
- Semi-core states are optional (for numerical stability) in Ce calculations, essential for numerical stability in Th calculations.

# Th DOS



DoS for Th  
Calculated at theoretical equilibria with AM05 using

- SR (black dotted)
- SO (blue dashed)

and

- Dirac (red solid)

Energies are relative to the Th  $5d_{5/2}$  core state which should reasonably be the same in all three calculations.

- In contrast to Ce, DOS don't consistently align. The  $5s$  are almost identical, but valence Dirac and SO are shifted relative to SR and Dirac and SO  $6p_{1/2}$  differ.
- SO is at a lower volume, with a more condensed density (and higher  $\nabla V$ ), and so, all else being equal, should be more split than Dirac.



# Consequences for heavy elements

Relativistic effects need to be incorporated via the Dirac equation.

When relativistic semi-core electrons are participating in the bonding, and thus need to be treated in the valence, there is no way around using the Dirac equation.

Adding Dirac p local orbitals to a scalar relativistic calculation, as done in some codes, might work but needs to be validated.

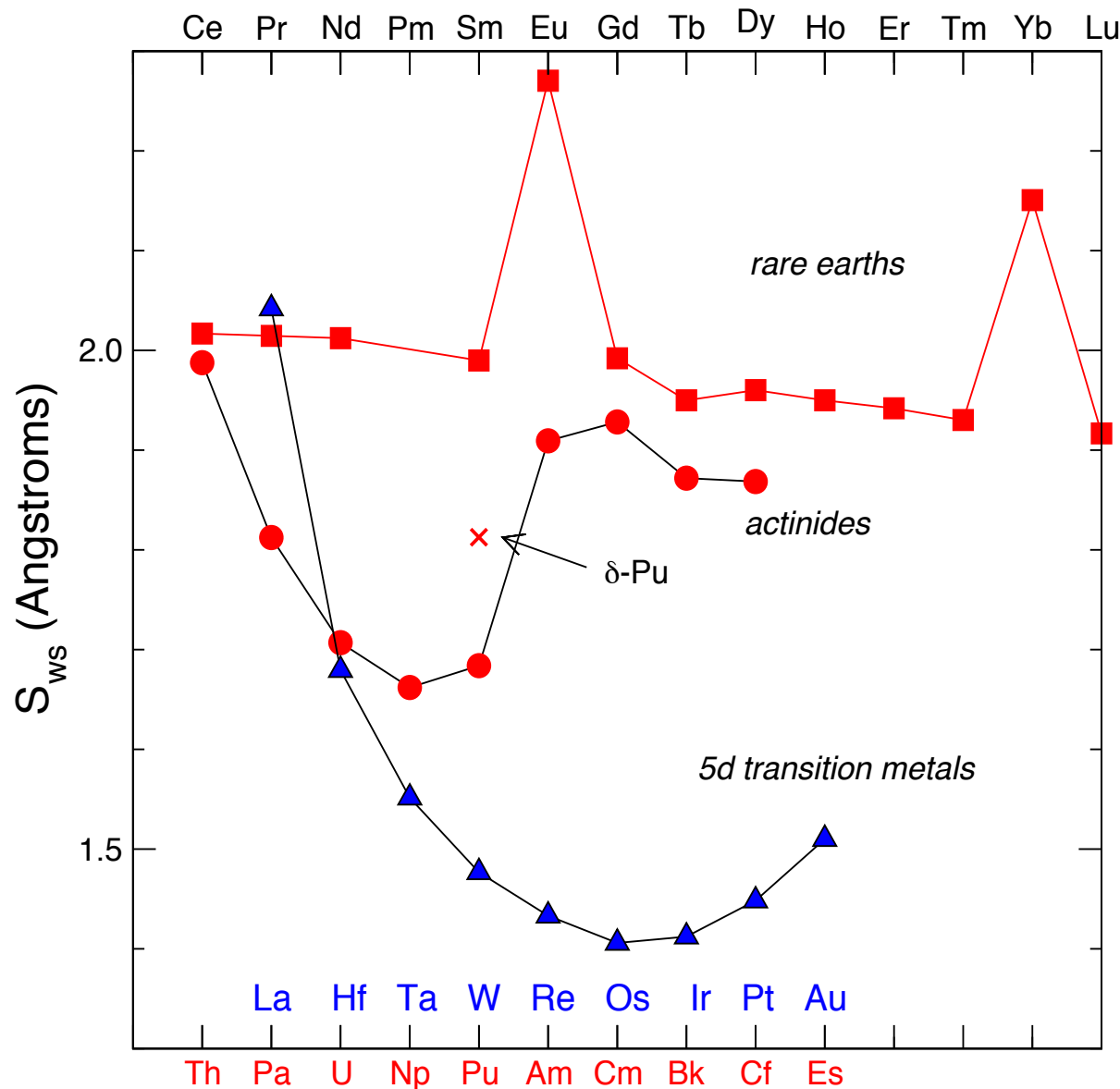
Simply removing the spin-orbit coupling on the 5p's, as is done in some other codes, is risky.

We can validate different treatments against Dirac results with the RSPt code.

Note: A cancellation of error in the variational spin-orbit coupling calculation makes the PBE functional give 'the right result'.

Which leads us into the next topic:

# Confinement physics



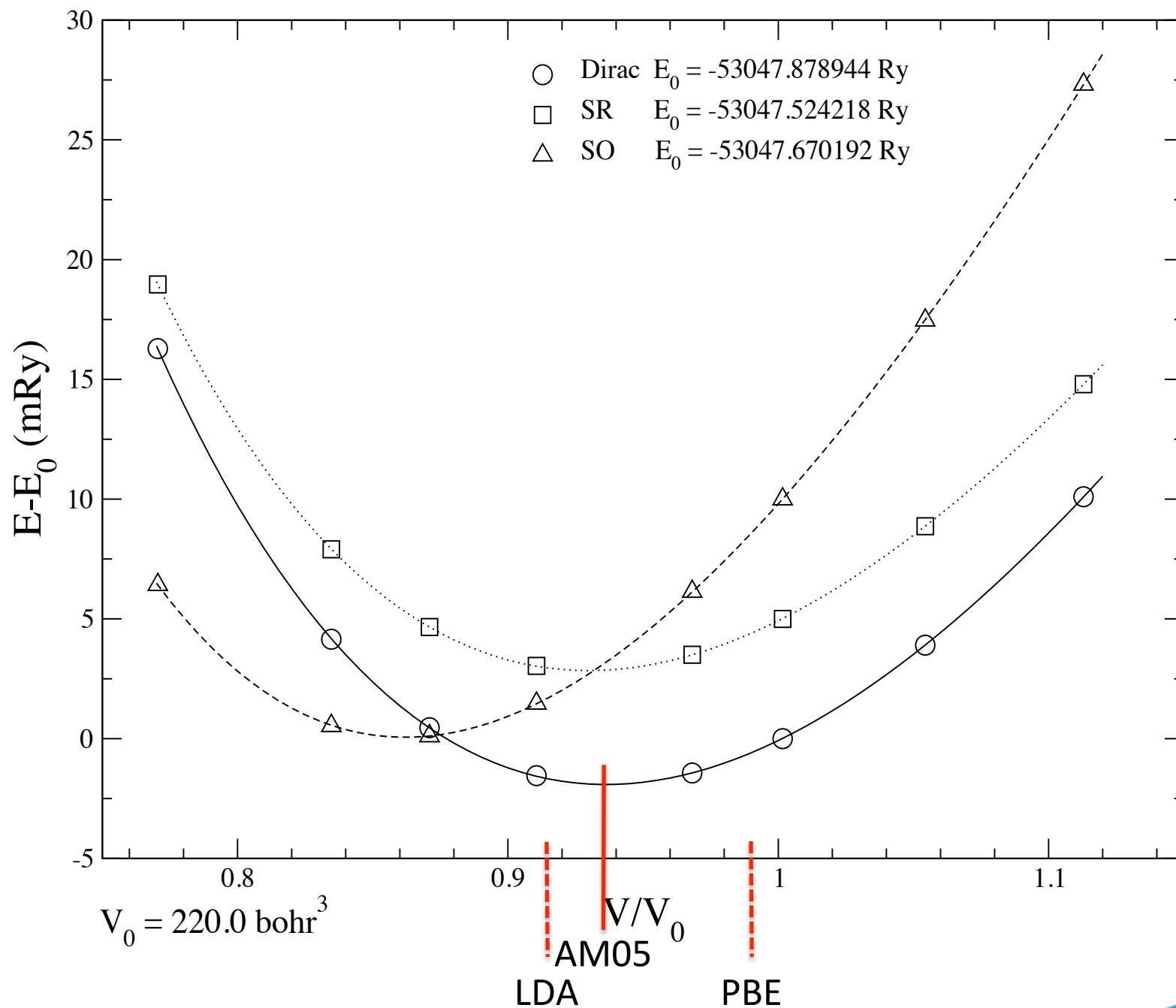
J M Wills and Olle Eriksson, Phys. Rev. B 45, 13879 (1992)

Experimental equilibrium volumes.

✧ LDA/AM05/PBE work reasonably well for **5d transition metals** (-2%/0 %/+2 %), but, contrary to experiments, give the same parabolic trend for **rare earths** and **actinides**.

✧ Dirac treatment not likely to change this dramatically.

# Thorium AM05 results



# Summary Thorium

TABLE I: Thorium equilibrium volumes in cubic bohrs and bulk moduli in GPa calculated with scalar relativistic, scalar relativistic with variational spin-orbit, and full Dirac methodologies, using AM05<sup>17</sup>, PBE<sup>2</sup>, and PW<sup>18</sup> functionals as described in the text. The zero temperature experimental volume, with zero point motion subtracted, is 220.00 bohr<sup>3</sup><sup>13</sup>. Reference 13 gives 205.14 for AM05. 218.02 for PBE, and 200.89 for PW.

	V/a <sub>0</sub> <sup>3</sup>			B (GPa)		
	AM05	PBE	PW	AM05	PBE	PW
Scalar Relativistic	204.55	217.36	199.89	58.9	54.5	65.5
Scalar Relativistic+Spin Orbit	189.62	201.21	186.45	74.1	68.6	80.4
Full Dirac	205.98	217.98	201.54	62.4	58.3	68.0

Note: PBE is giving 7% too large volume for gold. Generally underbinding.  
 “When PBE gets the right equilibrium volume, you should get suspicious”.  
 Seen like an indication that a hybrid functional or exact exchange is needed.  
 Confinement physics...

# Confinement error and Harmonic Oscillator model (HO)

Hao, Armiento and Mattsson  
Phys, Rev. B **82**, 115103 (2010).

Ann E Mattsson

HO model: Localized electron levels in a continuum.

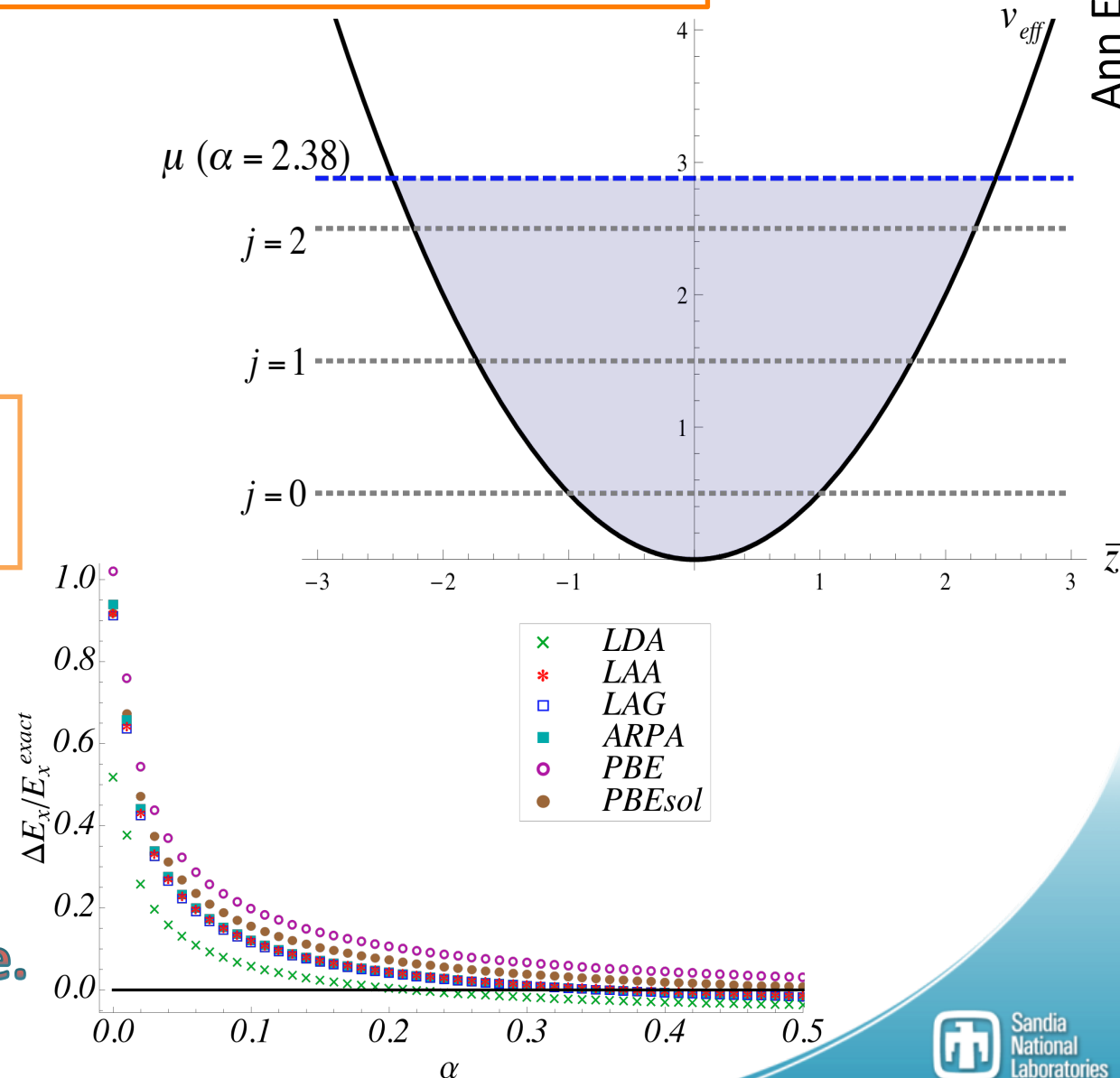
Energy of subbands  $\varepsilon_j = (j + \frac{1}{2}) \frac{1}{l^2}$

Chemical potential  $\mu = (\alpha + \frac{1}{2}) \frac{1}{l^2}$

$\alpha$  characterizes how many subbands have been occupied, and determines the level of confinement.

Relative errors of  $E_x$  of the HO gas introduced by different functionals.

**As  $\alpha$  decreases, the confinement errors increase.**





# Electron localization function (ELF)

A.D. Becke and K. E. Edgecombe, J. Chem. Phys. **92**, 5397 (1990)

$$ELF = \frac{1}{1 + (D/D_h)^2}$$

$$D = \tau - \frac{1}{8} \frac{|\nabla n|^2}{n}$$

$$D_h = \frac{3}{10} (3\pi^2)^{2/3} n^{5/3}$$

$\tau$ : kinetic energy density

$n$ : electron density

$D$ : kinetic energy excess with respect to a boson gas.

$D_h$ : kinetic energy of a uniform electron gas.

ELF  $\approx$  1/2: uniform electron gas like

ELF  $\approx$  1: strong localization

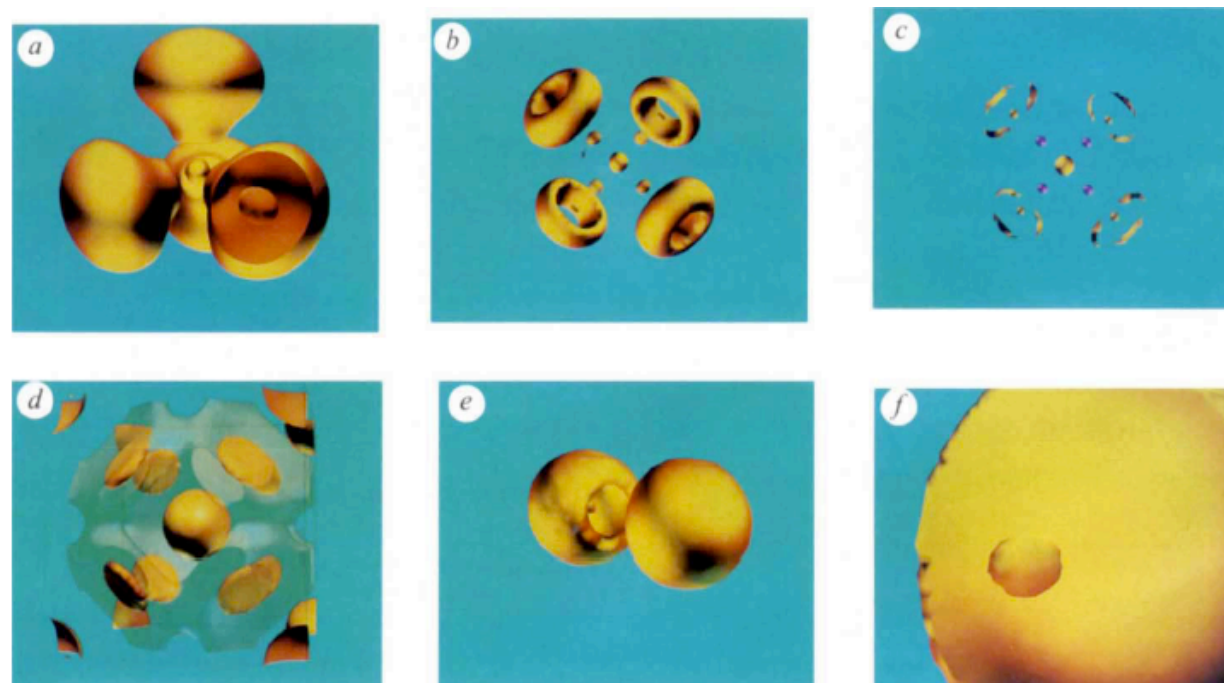


FIG. 1. Localization domains of  $CF_4$  (a-c), Li (d), LiF (e) and LiH (f). a-c, Reduction of the localization domains of  $CF_4$ . Below ELF=0.37 (where ELF is the localization function; see text) there are six localization domains: five core and one valence. The bifurcation at ELF=0.37 splits the common valence domain into four atomic ones. The ELF=0.75 map (a) shows the carbon core surrounded by the four fluorine valence domains; the front cutting plane has been chosen so that a fluorine core domain can be seen. The bonding attractors are responsible for the bulges towards the carbon centre. A further bifurcation occurs at ELF=0.78, giving rise to bonding point attractors and non-bonding ring attractor domains as shown in b (ELF=0.85). Each ring is itself resolved into three non-bonding point attractors for ELF>0.883. In c, the bonding attractors at which ELF=0.879 are represented by purple spheres because the bounding isosurface 0.885 only encapsulates the core and non-bonding attractors. b.c.c. lithium: the core and bonding attractors are located at the 8a (centre and vertices of the cubic lattice) and 8c

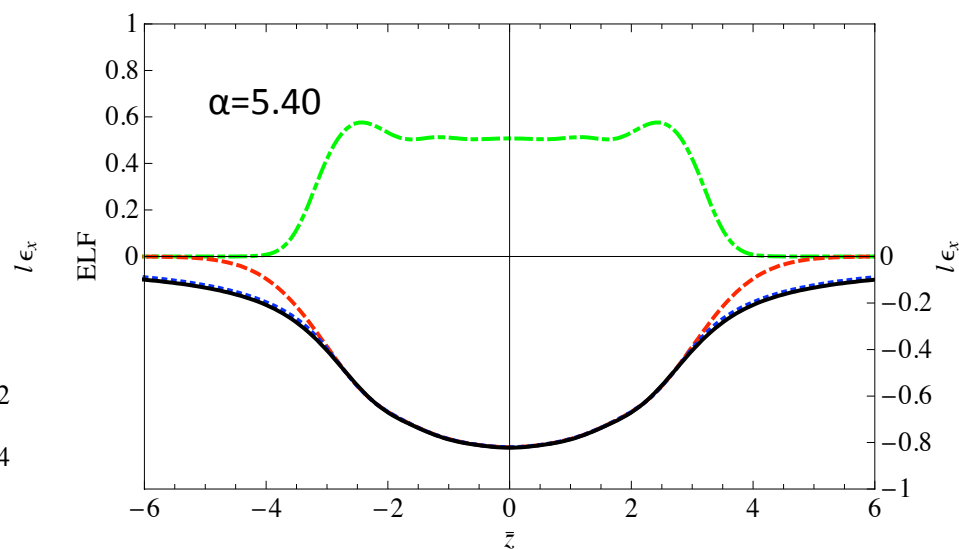
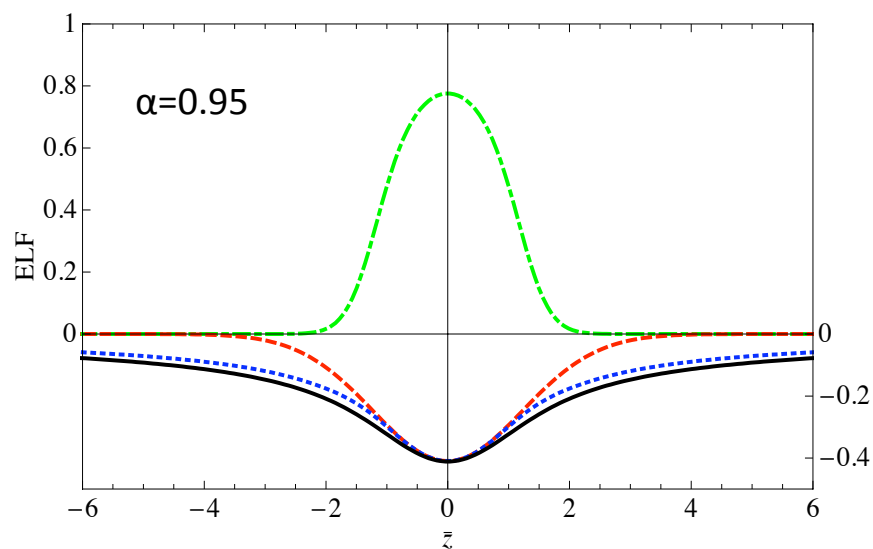
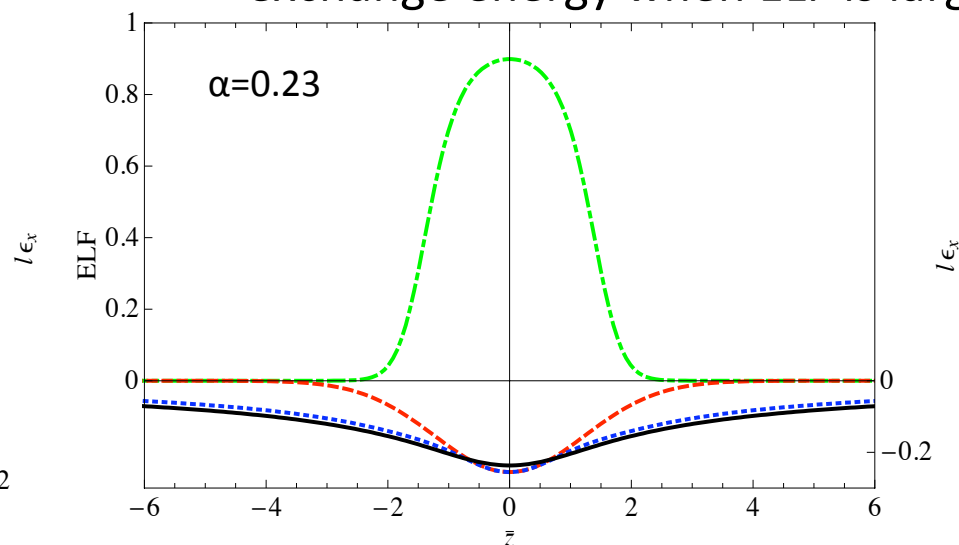
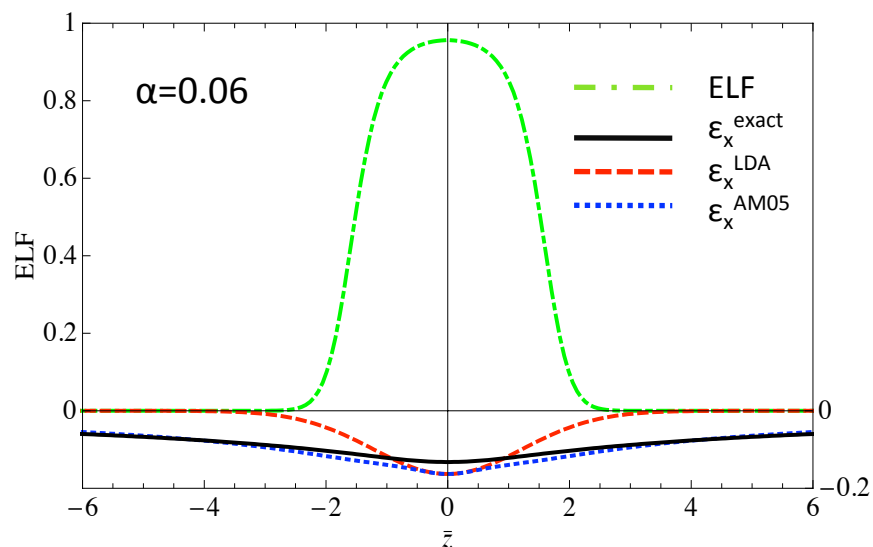
(midpoints between the centre and the vertices) positions respectively. Their domains are bounded by the ELF=0.625 isosurfaces, and the ELF=0.575 isosurface forms a network of channels connecting the bonding attractors. These bonding attractors are unsaturated because there are eight per cell sharing two valence electrons. For LiF e, the localization domains shown are bounded by the ELF=0.84 isosurface. The fluorine valence domain (which is almost spherical at lower ELF values) shows a hole in front of the lithium core; increasing the threshold leads to a single attractor lying on the internuclear axis on the side of the fluorine core that is away from the lithium. The ELF=0.999 isosurfaces of LiH (f) encapsulate, on the one hand, the lithium core and, on the other hand, a very large area which extends, in principle, to infinity. The calculation of the grid points has been limited to a box of dimensions  $7 \times 7 \times a.u.$ , therefore only one face of the largest domain can be seen. The roughness of the surface is due to interpolation limitations and a density cutoff.

B. Silvi and A. Savin, Nature **371**, 683 (1994)

# Confinement error and ELF

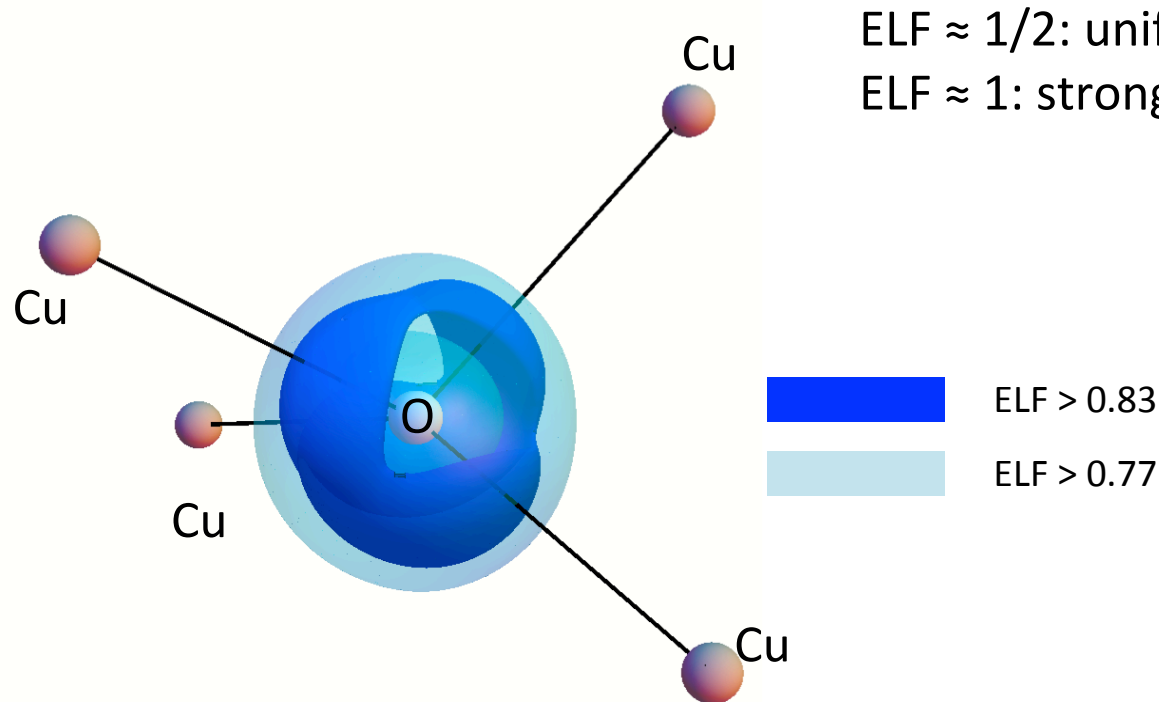
HO systems:

Note, all functionals give too negative exchange energy when ELF is large.



**ELF is correlated with the confinement errors!**

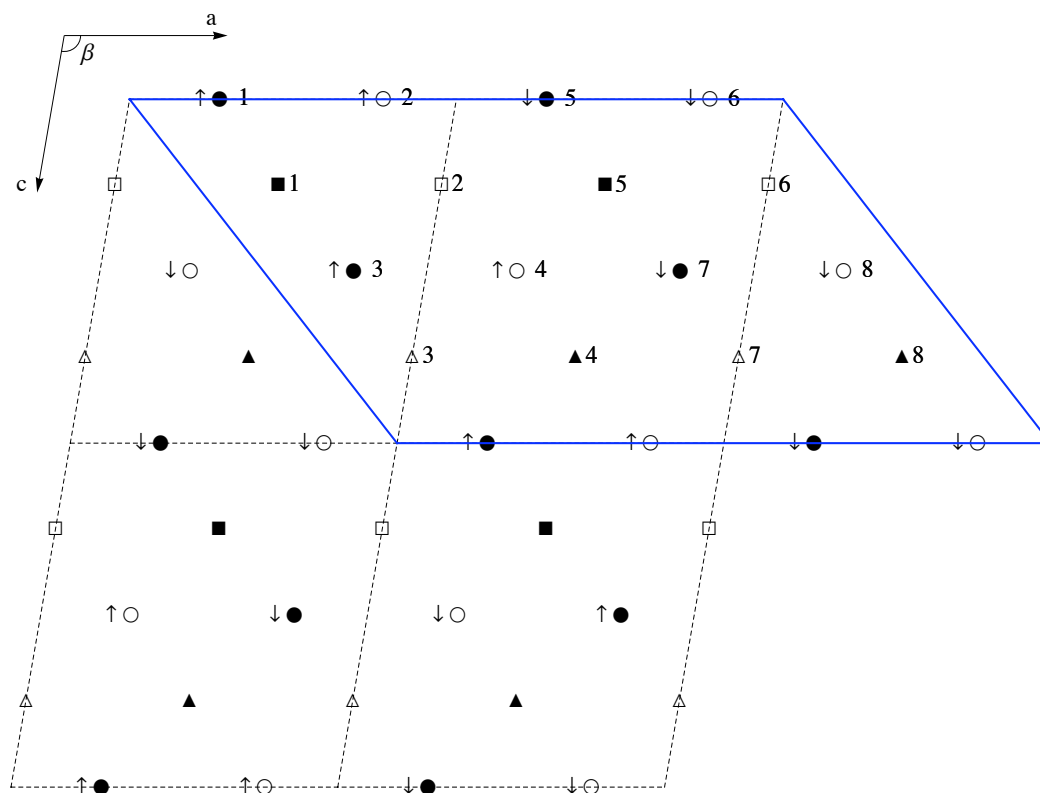
# ELF in a 'real' system: CuO



CuO: Monoclinic structure obtained when starting from the experimental structure with each dimension scaled by 3%

The high ELF regions are around the oxygen atoms. We identify these as the regions where hybridization in solid materials occur.

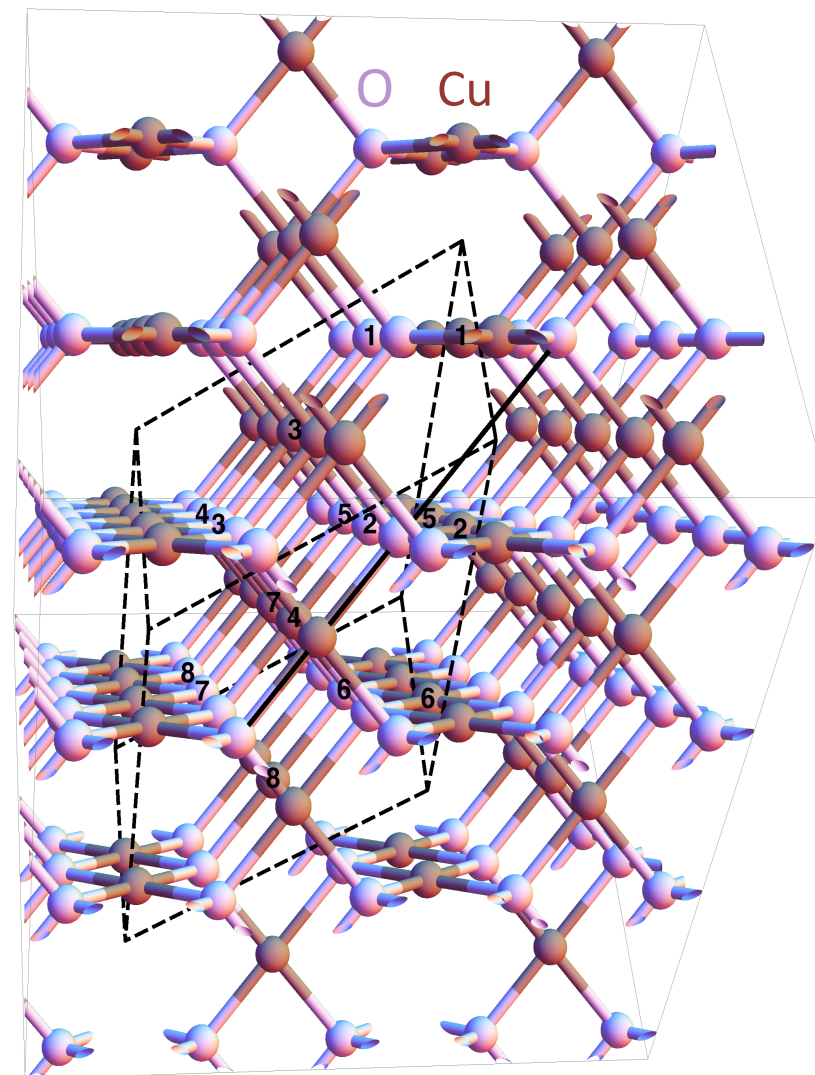
# Experimental structure of CuO



- Cu  $y = 1/4$
- Cu  $y = 3/4$
- O  $y = 1/2+u$
- O  $y = u$
- ▲ O  $y = 1/2-u$
- △ O  $y = 1-u$
- ↑↓ spins

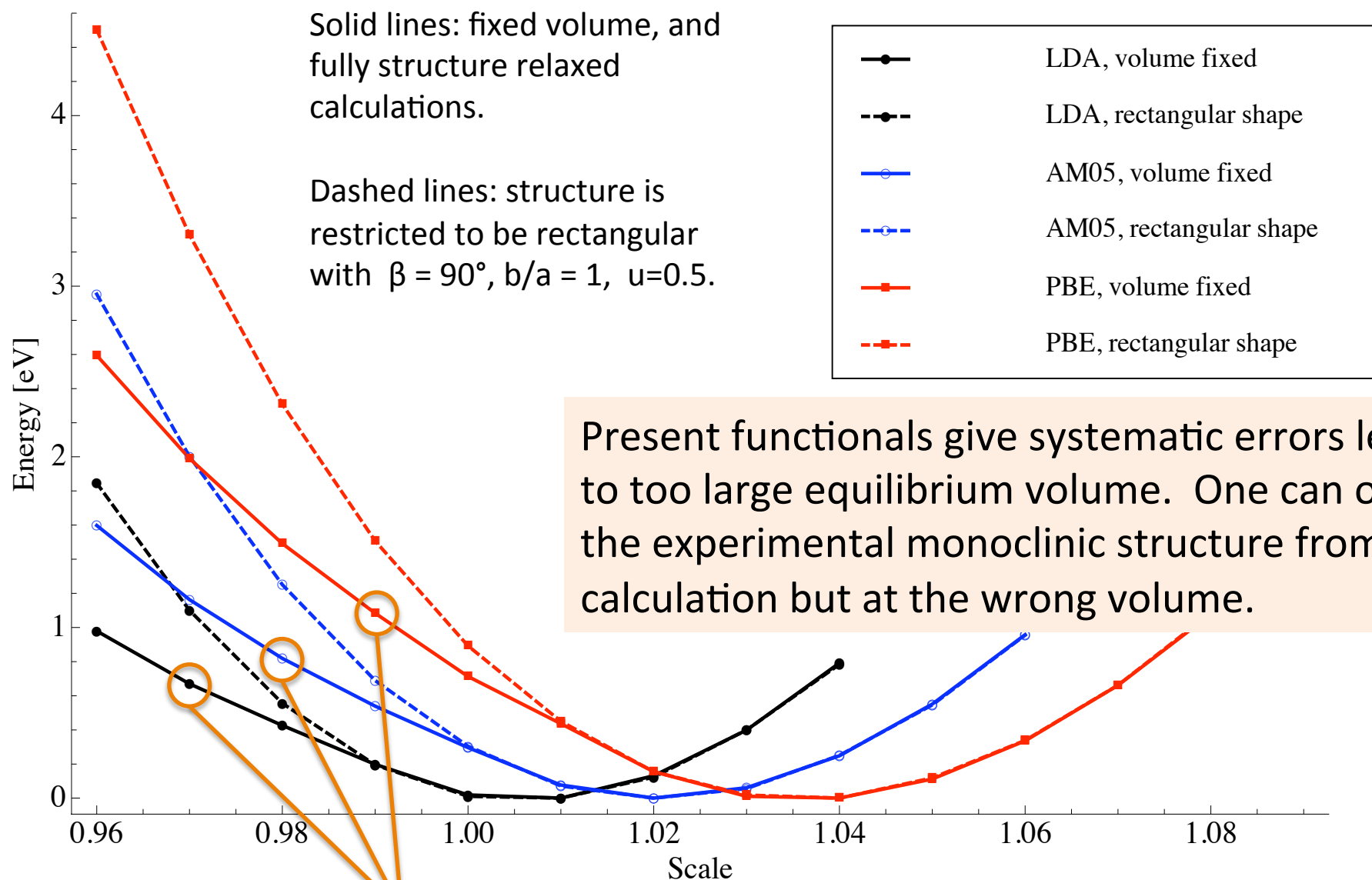
Experimental lattice parameters:

$a = 4.6837 \text{ \AA}$ ,  $b = 3.4266 \text{ \AA}$ ,  $c = 5.1288 \text{ \AA}$ ,  $\beta = 99.54^\circ$ ,  $u = 0.4184$



Rectangular shape obtained from DFT calculation.  
 $a = 4.0396 \text{ \AA}$ ,  $c/a = 1.23$ ,  $b/a = 1.0$ ,  $\beta = 90^\circ$ ,  $u = 0.5$

# DFT calculations of CuO structure



Present functionals give systematic errors leading to too large equilibrium volume. One can obtain the experimental monoclinic structure from DFT calculation but at the wrong volume.

Structures with relative dimensions close to the experimental structure are obtained in these points.

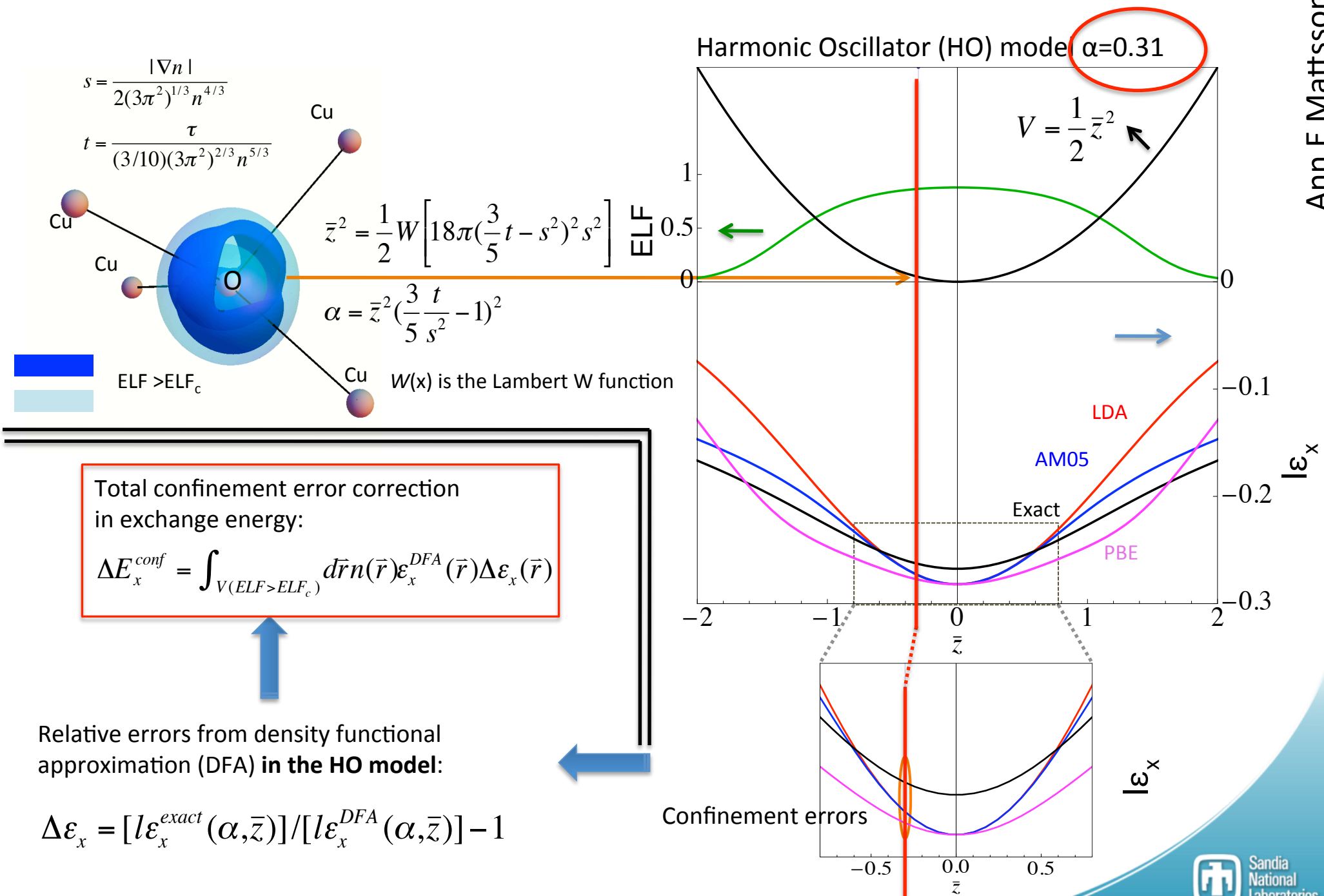
$$\text{Scale} = (V/V_0)^{1/3}$$

$V_0$  is the lattice volume of the experimental structure

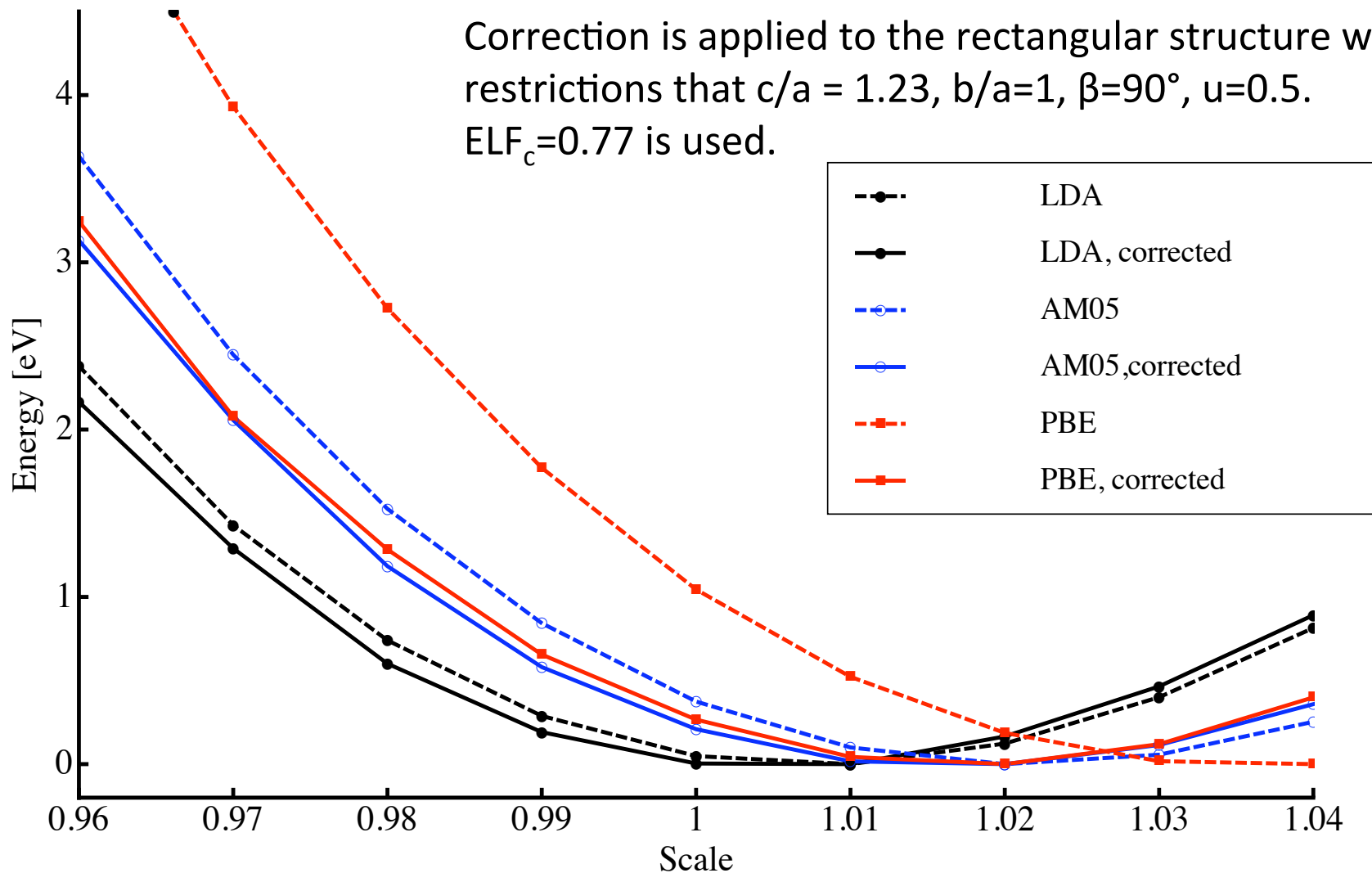


# Confinement error correction scheme

Ann E Mattsson



# Confinement error correction for CuO

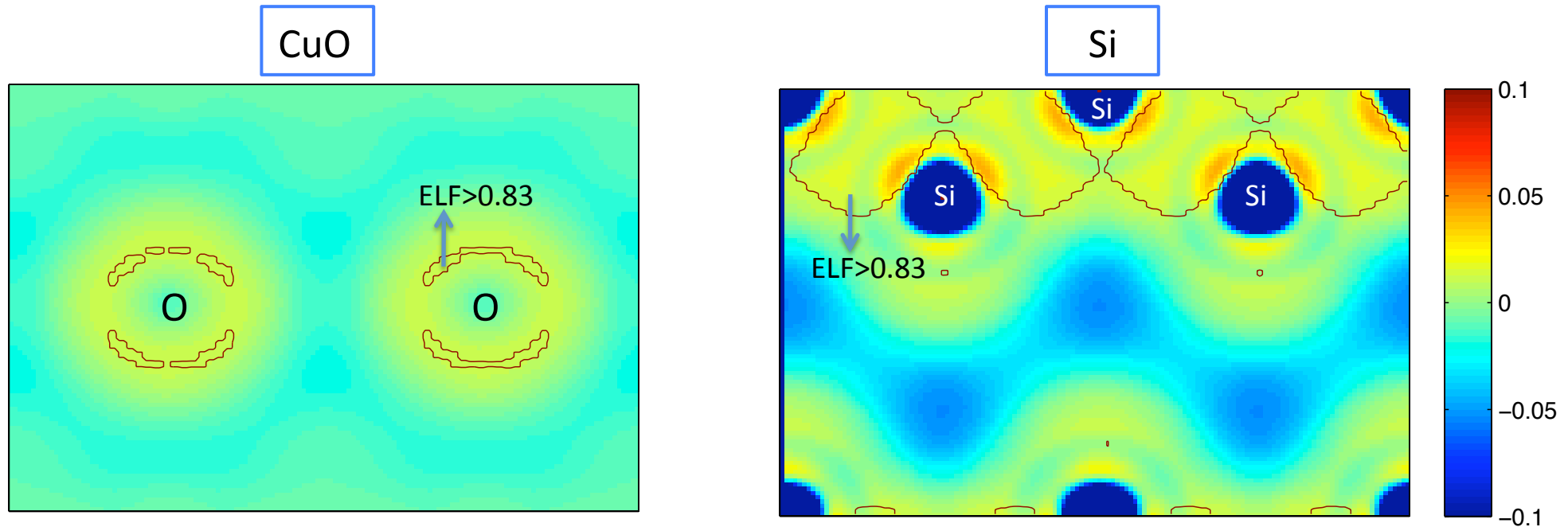


Equilibrium structure has been shifted to have smaller volume after correcting the confinement errors. AM05 and PBE have approximate same line shape after the correction.

# Self consistency needed for, for example, Si

Relative density difference between PBE and LDA calculation:

$$(n^{\text{PBE}} - n^{\text{LDA}}) / n^{\text{LDA}}$$



Ann E Mattsson

Density difference obtained from different functionals are larger in Si than in CuO.

The confinement errors have to be treated self-consistently for Si.

# Si from QMC

ANTONIO C. CANCIO AND M. Y. CHOU

PHYSICAL REVIEW B **74**, 081202(R) (2006)

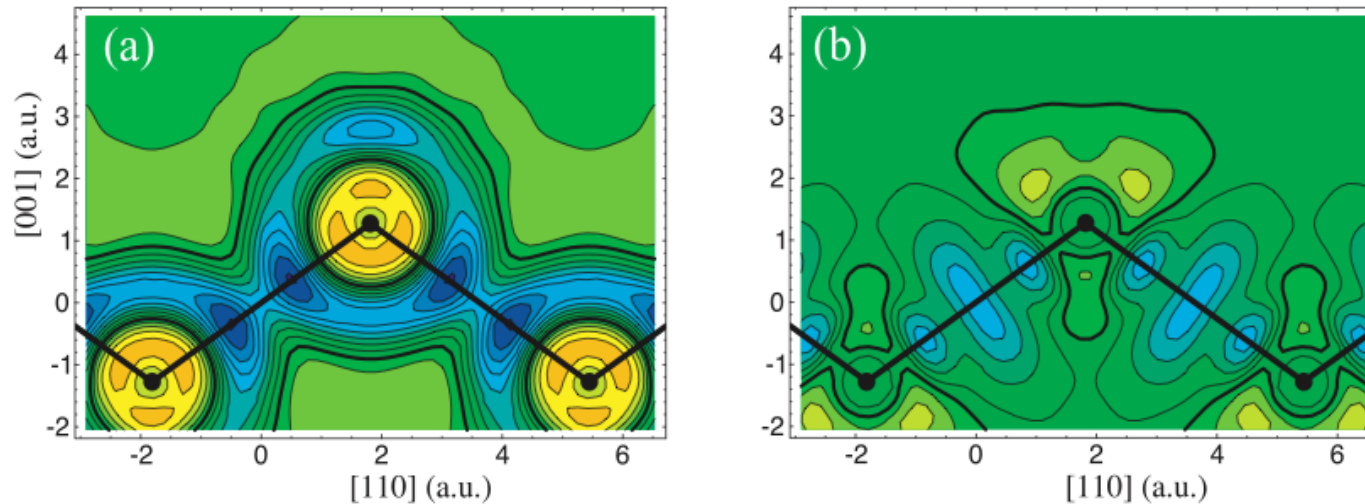
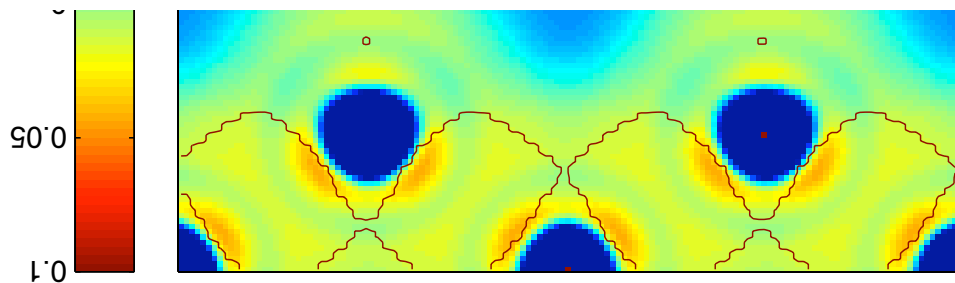


FIG. 1. (Color) Comparison of DFT and VMC  $e_{xc}$ 's on the (110) plane of the Si crystal. (a) Difference between the LDA  $e_{xc}$  and that of VMC data (Ref. 10). Difference between that of the GGA++ model described in the text and the VMC result. Contours in increments of  $0.2 \times 10^{-3}$  a.u., with thicker contour that for zero difference. Bluer (darker) regions show negative difference and redder (lighter) regions, positive.



# Si from QMC

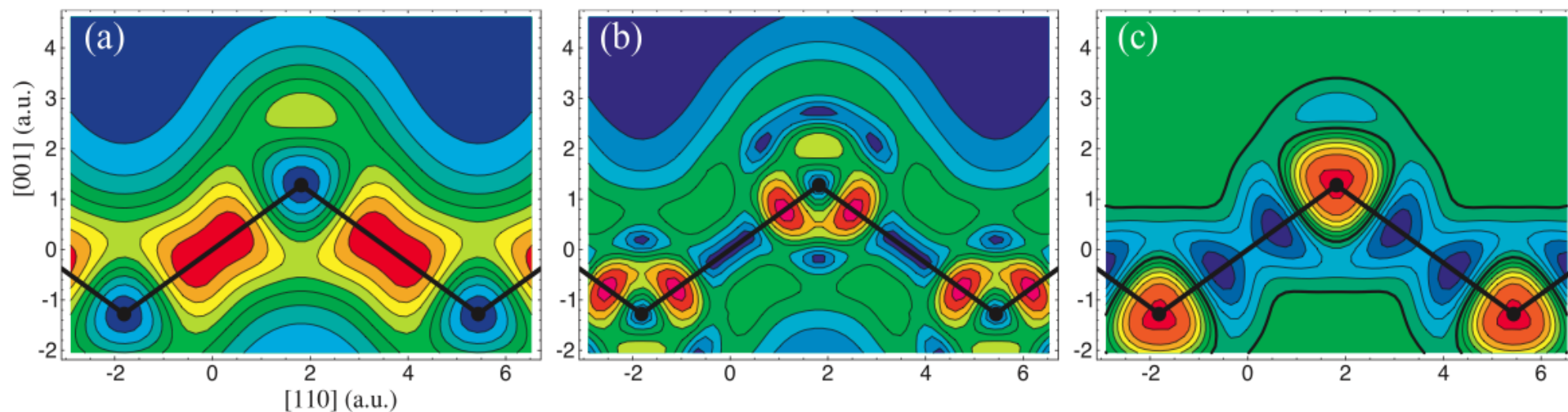
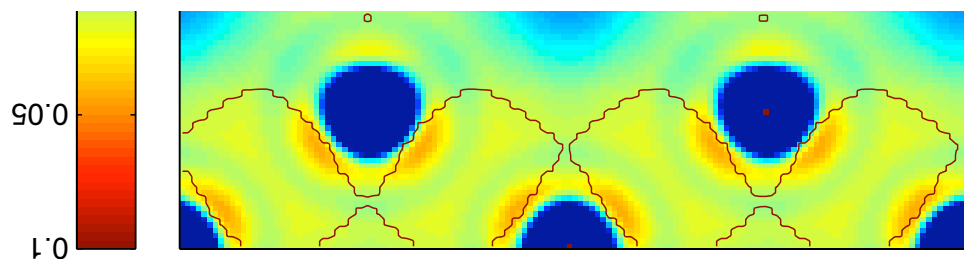


FIG. 2. (Color) Gradient analysis of the density of crystalline Si. The density  $n$  (a),  $|\nabla n|$  (b), and  $\nabla^2 n$  (c) on the (110) plane of the Si crystal. Atoms and bonds outlined in black. Shading varies from blue (dark gray) (low) to red (light gray) (high) and contours are in increments of 0.01 (a), 0.01 (b), and 0.05 a.u. (c). In (c) the zero contour is the thicker black line.



# Subsystem functionals

From  
general purpose functionals  
to  
specialized functionals

$$E_{xc} = \int_V n(\mathbf{r}) \epsilon_{xc}(\mathbf{r}; [n]) dV$$

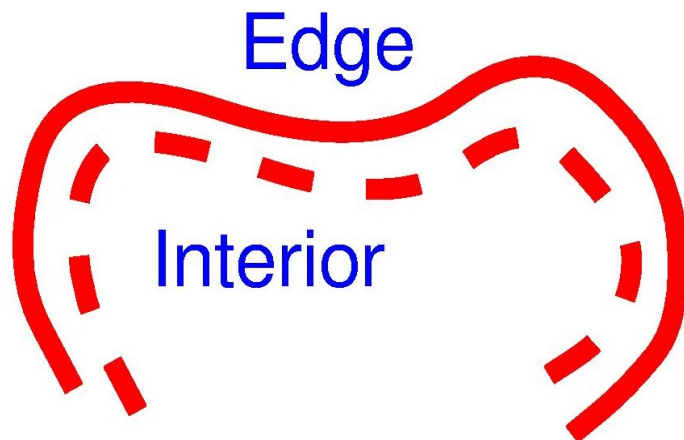
Use specialized functionals  
in the different subsystems

Divide integration over  $V$   
into integrations over subsystems



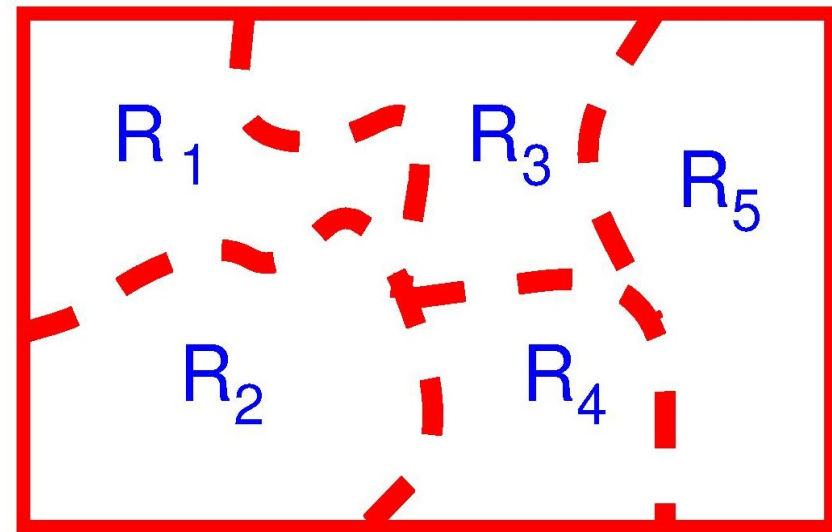
# Subsystem functionals

## Original Kohn and Mattsson approach



Kohn, Mattsson PRL 81, 3487 (1998)

## Generalized Idea



Every subsystem functional is designed to capture a specific type of physics, appropriate for a particular subsystem.

# LDA and Ceperly-Alder

Ceperly and Alder, PRL 45, 566 (1980).

Quantum Monte Carlo calculations of the ground-state energy of uniform electron gases (model systems) of different densities.

Most correlation functionals in use today are based on their data.

ALL LDA correlation functionals in common use are based on (fitted to) their data.

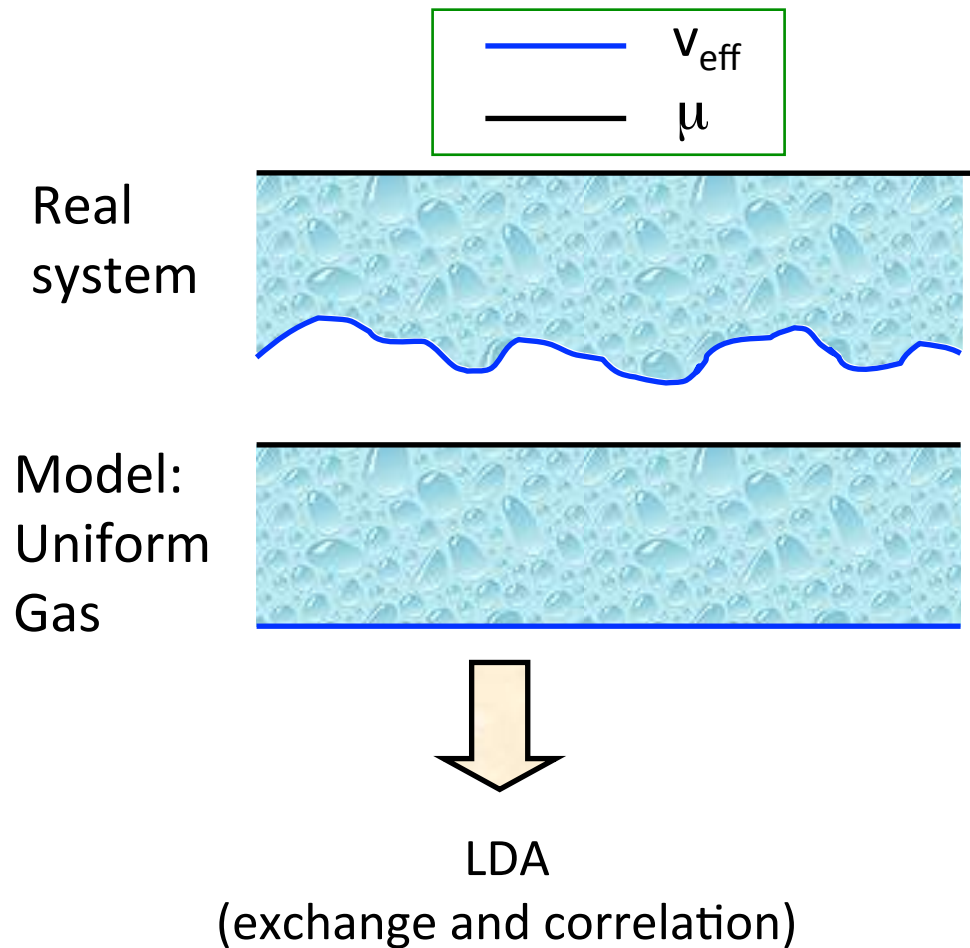
(Before 1980, for example, Wigner correlation was used)

Total energy – energies from known formulas = Exchange-correlation energy.

From SE

From DFT

# The LDA functional



Assume each point in the real system contribute the amount of exchange-correlation energy as would a uniform electron gas with the same density.

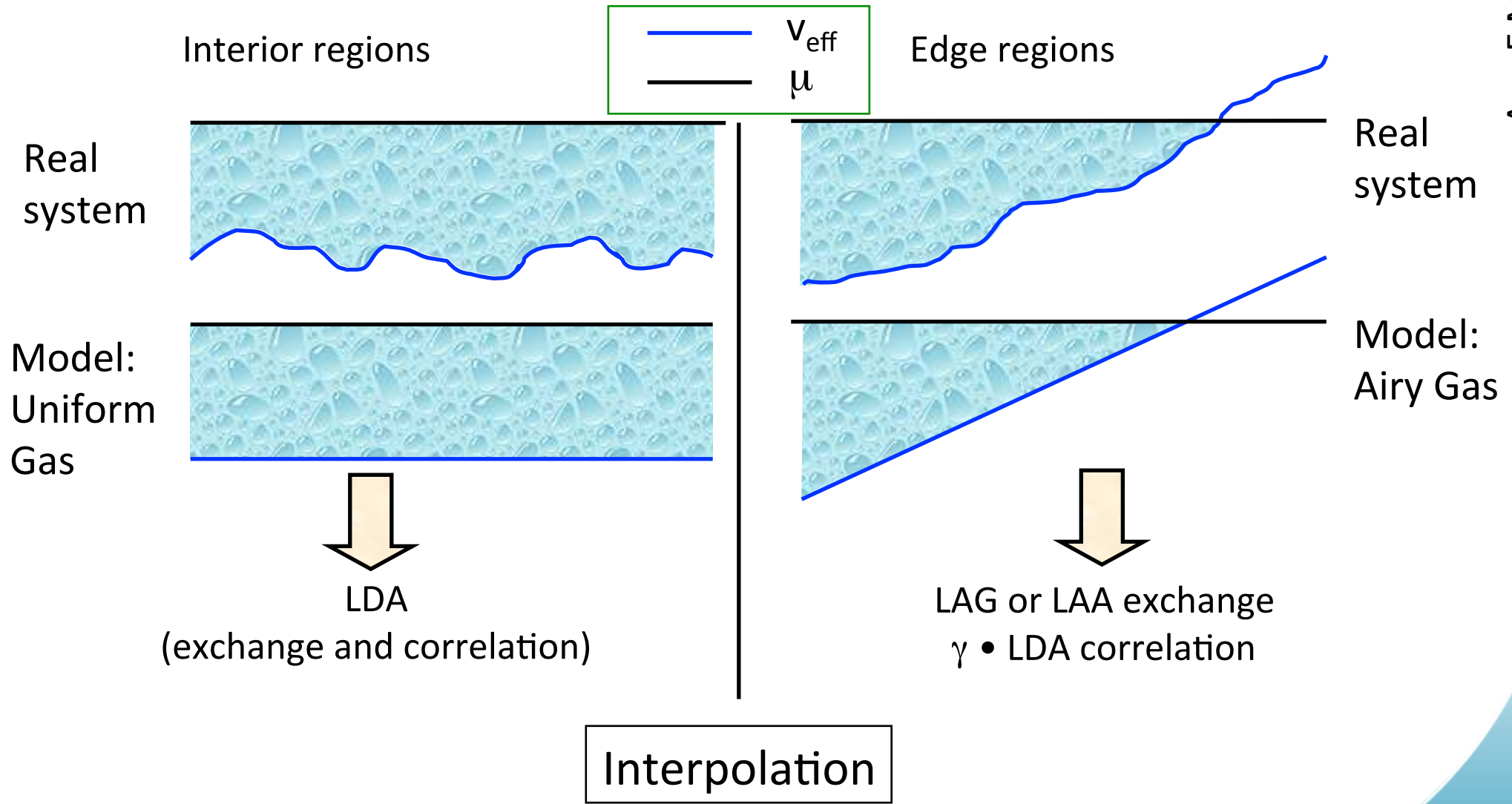
Obviously exact for the uniform electron gas.

Basic concept and first explicit LDA published in 1965 (Kohn and Sham).

# General functional from subsystem

## functionals: AM05, PRB 72, 085108 (2005)

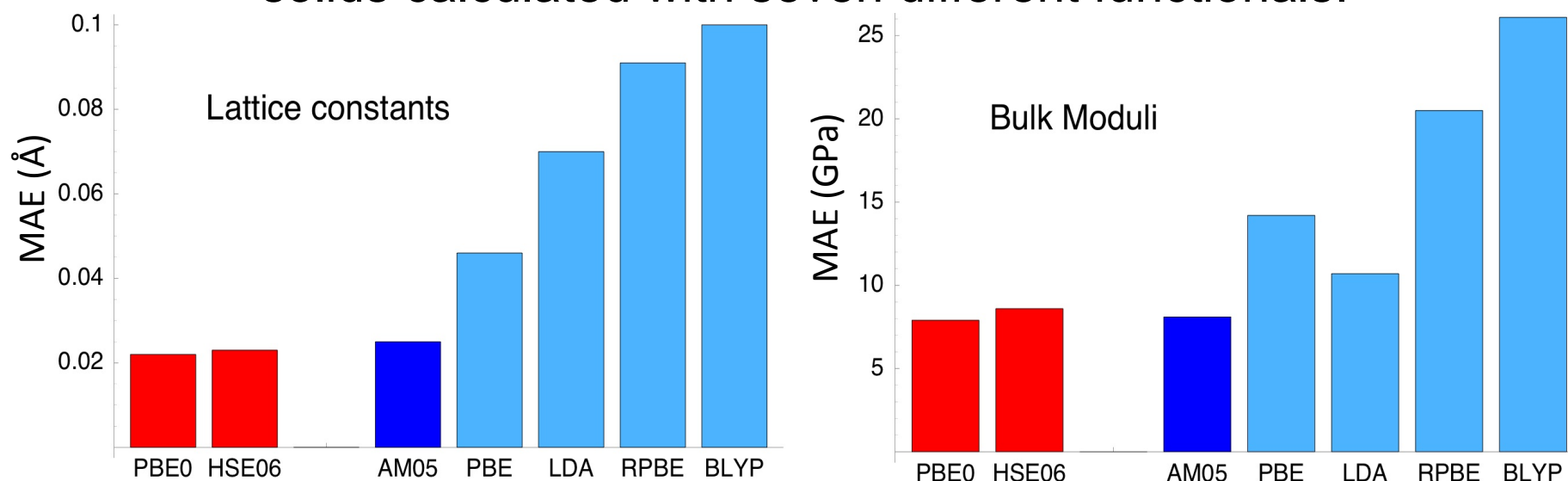
Ann E Mattsson



Two constants (one is  $\gamma$  above, one is in interpolation index) are determined by fitting to yield correct jellium surface energies.

# AM05 is as accurate as a **hybrid**, but much faster

Comparison of mean absolute errors (MAE) for properties of 20 solids calculated with seven different functionals.



GGA type functionals (**blue**) are one to three order of magnitudes faster to use than **hybrids** (**red**). **AM05** has the same accuracy as **hybrids** for solids and thus enable accurate and fast DFT calculations of, for example, defects in semi-conductors. It also allows for the use of DFT-MD as an accurate tool in EOS construction.

**AM05 also proves that fast AND accurate is possible.**

# What is next?

The construction of AM05 shows that the subsystem functional scheme can be a fruitful way of constructing exchange-correlation functionals.

We want to use this scheme for developing a general functional that can also give good results for some systems that presently available functionals have problems with:

- Systems with ‘localized’ electrons, such as transition metal oxides and actinides.
- Systems where van der Waals’ forces dominate the physics.



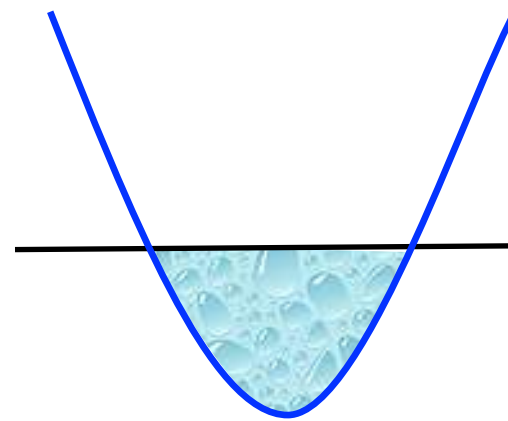
# Subsystem Functional Scheme:

$$E_{xc} = \int_V n(\vec{r}) \varepsilon_{xc}(\vec{r};[n]) dV$$

Dividing V into sub-regions where different subsystem functionals apply

Specialized functionals in different subsystems

Confinement physics:  
Harmonic oscillator gas

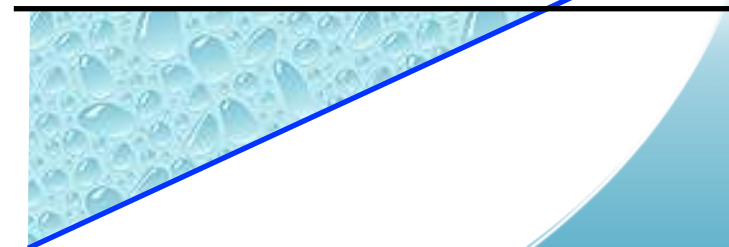


Interior physics:  
Uniform electron gas



Interpolation  
Index:  
ELF?

Surface physics:  
Airy Gas



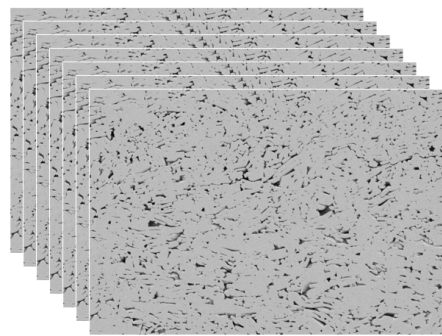
# We want to be able to do DFT based calculations for all materials

While DFT is very successful for many materials and many properties, not all materials and properties are equally well treated with DFT. This is the case with, for example, equilibrium properties of explosives.

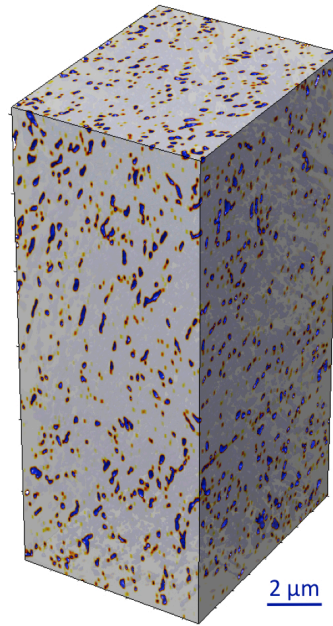
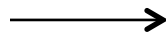
We have one problem:

- The van der Waals' forces

# The Future: Hydrocode simulations with explicit microstructure

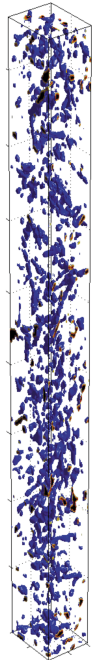
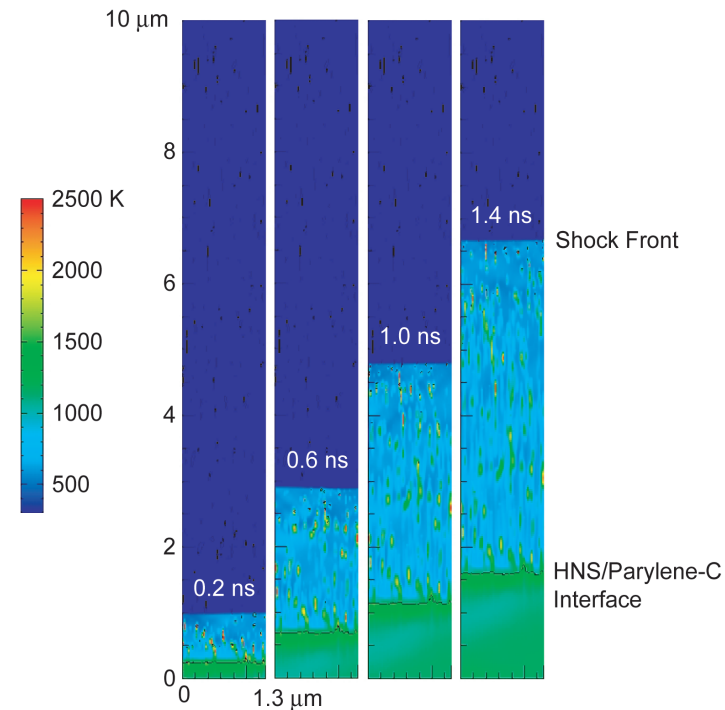


Nanotomography: 25 nm slices



80,000 pores

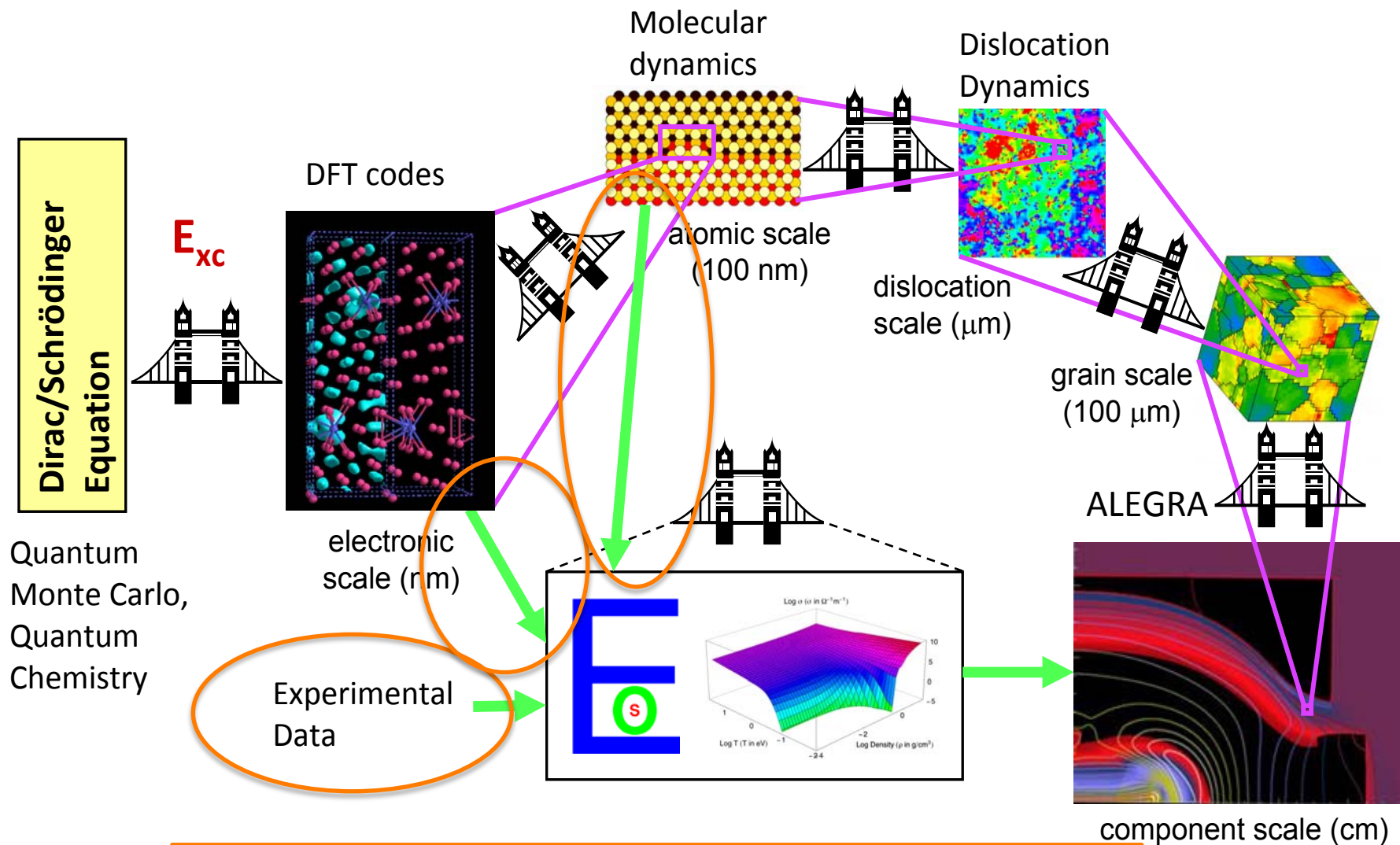
R.R. Wixom et al. J. Mater. Res. 25 (2010) 1362



Ann E Mattsson

Single crystal Equation  
of State needed.

# Bridges between Fundamental Law of Nature and Engineering



The ability to perform high-fidelity calculations is most important for cases where experiments are impossible, dangerous, and/or prohibitively expensive to perform.

# PETN: The bad news: Equilibrium structure

Functional	a (Å)	c/a	Comment
LDA	8.961	0.710	
HSE	9.69	0.718	estimated
PBE	9.888	0.718	
AM05	---	---	no binding
Experiment	9.38	0.715	at ~298K

LDA, PBE, AM05: Energies calculated in a grid of 0.1 Å spacing in a and 0.01 spacing in c/a, extending at least 4 points on each side of minima (AM05 covering the PBE minima).

HSE: Because of the computational cost only three energies are calculated, from which the lattice parameter is estimated.

## Van der Waals'

HAAS, TRAN, AND BLAHA  
PHYSICAL REVIEW B **79**, 085104 (2009)

TABLE III. Equilibrium lattice constant (in Å,  $a_0$  for Ne and Ar, and  $c_0$  for graphite). The Strukturbericht symbols are indicated in parenthesis.

Method	Graphite (A9)	Ne (A1)	Ar (A1)
LDA	6.7	3.9	4.9
SOGGA	7.3	4.5	5.8
PBEsol	7.3	4.7	5.9
PBE	8.8	4.6	6.0
WC	9.6	4.9	6.4
TPSS	>15	4.9	6.4
AM05	>15	>5.5	>6.7
Expt.	6.71 <sup>a</sup>	4.47 <sup>b</sup>	5.31 <sup>b</sup>

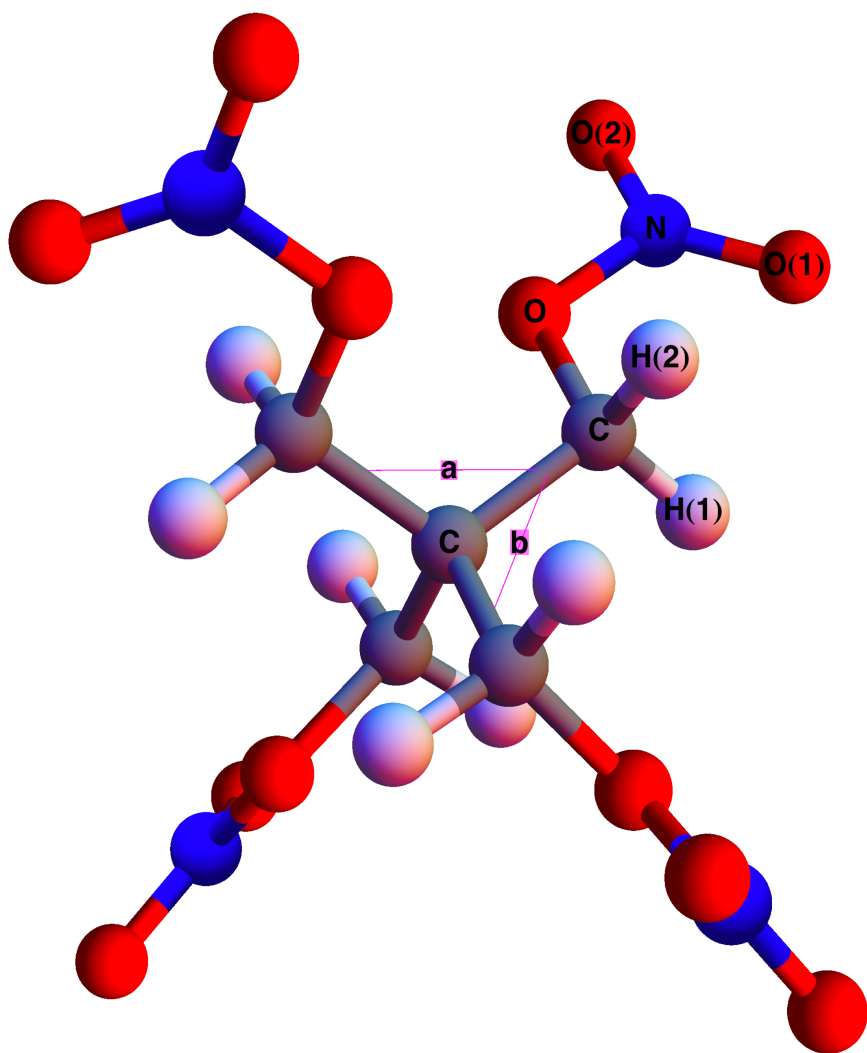
<sup>a</sup>Reference 76.

<sup>b</sup>References 77–79.

- LDA sometimes gives good minimum but for the wrong reasons, and not consistently.
- AM05 might be better off than other functionals since it contains no van der Waals', not even faulty.

PETN:

## The good news: Intramolecular structure



- We have calculated the molecule structure (bond lengths and angles) in the crystal environment.
- Functionals follow the usual trends but all give a good description compared to experiments.
- The large differences in equilibrium volumes thus stem from the poor description of the intermolecular van der Waals' bonds.



# Hugoniots: Circumvent problems at equilibrium

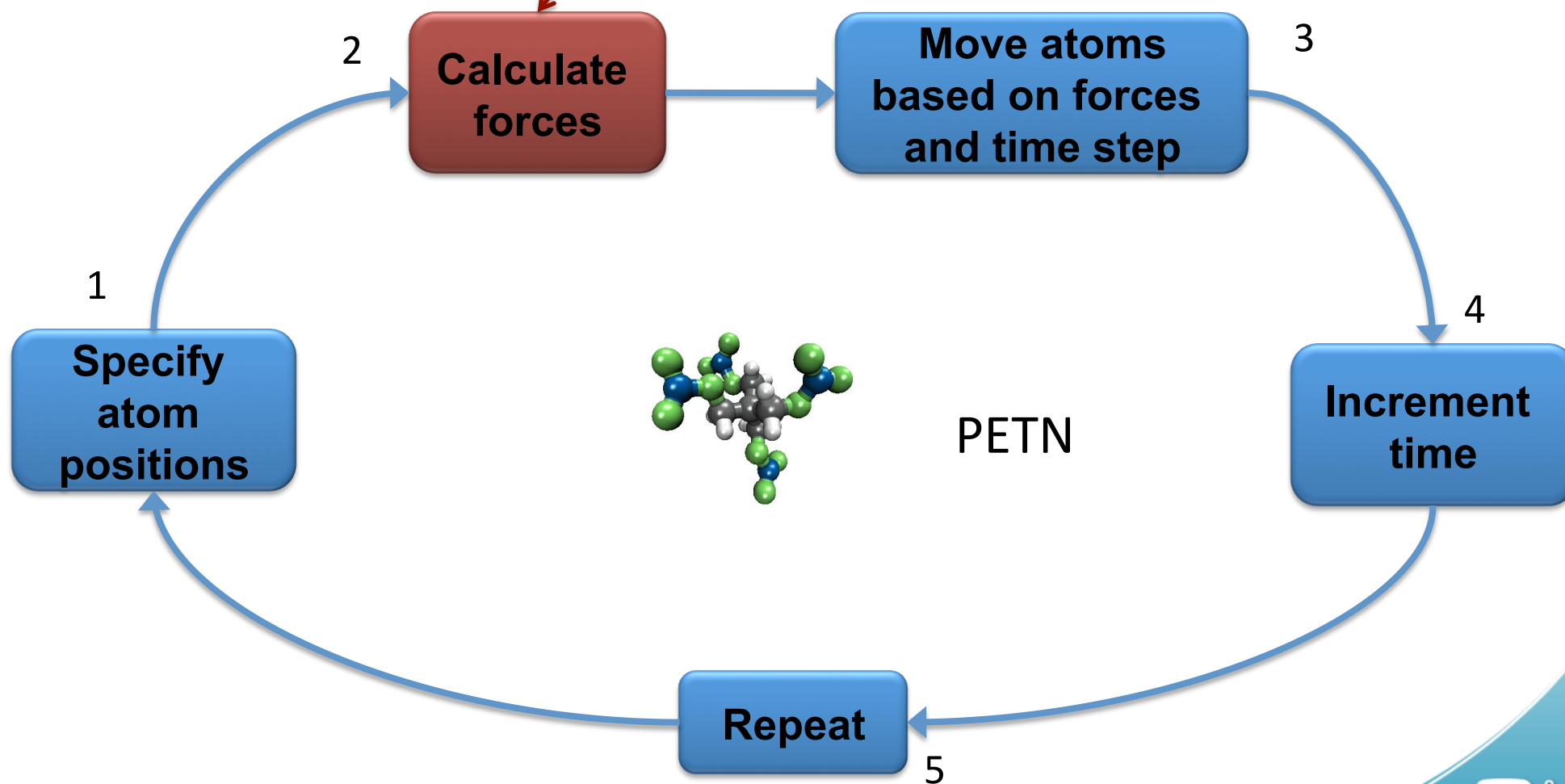
So, we know AM05 does not include any van der Waals' forces but that it treats compressed matter very accurately.

Idea: Use experimental equilibrium volume for the ambient reference but use the theoretical pressure at this volume (and room temperature) as pressure reference. (This methodology has been used for polymers before: AM05 does not bind any of them. However, the effect is small in the polymers, that is, the theoretical pressure is small).

Easy to motivate this using AM05, but harder when you have a functional that gives a faulty minima.

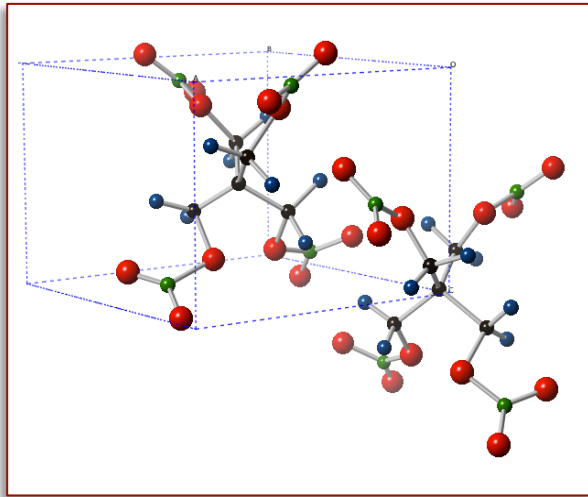
# Molecular Dynamics

DFT-MD (or a AIMD or QMD): Forces calculated with DFT.  
Classical MD: Forces calculated with force fields or potentials.

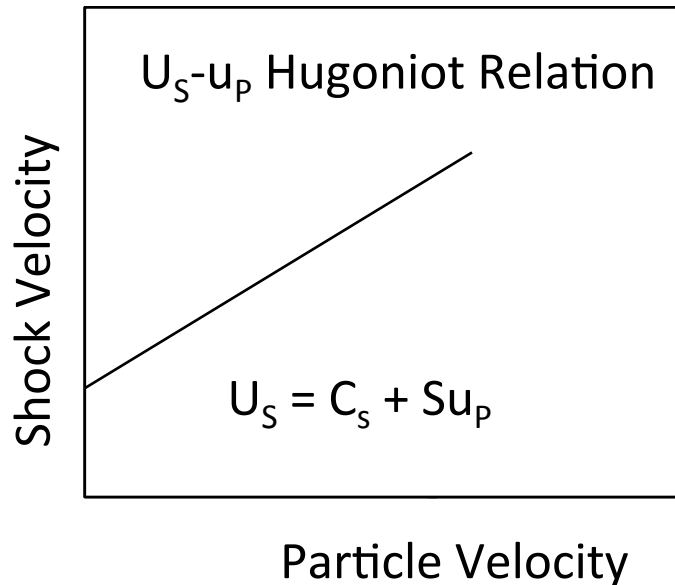
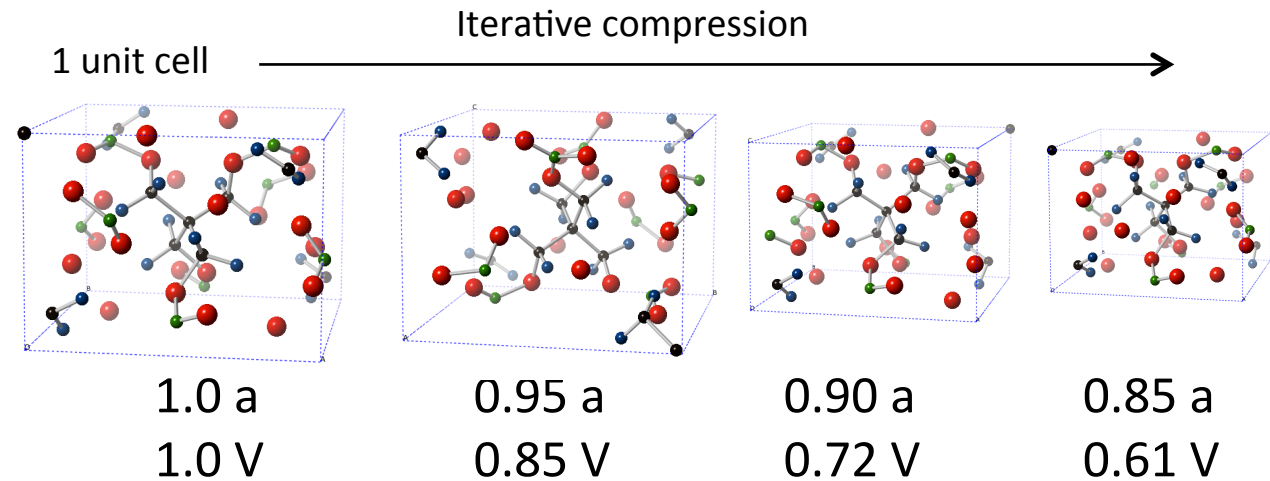


Adapted from slides by Ryan Wixom, SNL.

# Finding the Hugoniot State (P,T,E) for any V.



PETN,  $V_0$  at 300K



Mass

$$\rho_0 D = \rho_1 (D - u_1)$$

Momentum

$$P_1 = \rho_0 D u_1$$

Energy

$$E - E_0 = \frac{1}{2}(P + P_0)(V_0 - V) \quad \text{R.H. equation}$$

**Key Point:** jump conditions are only valid on the Hugoniot

Approach 1:

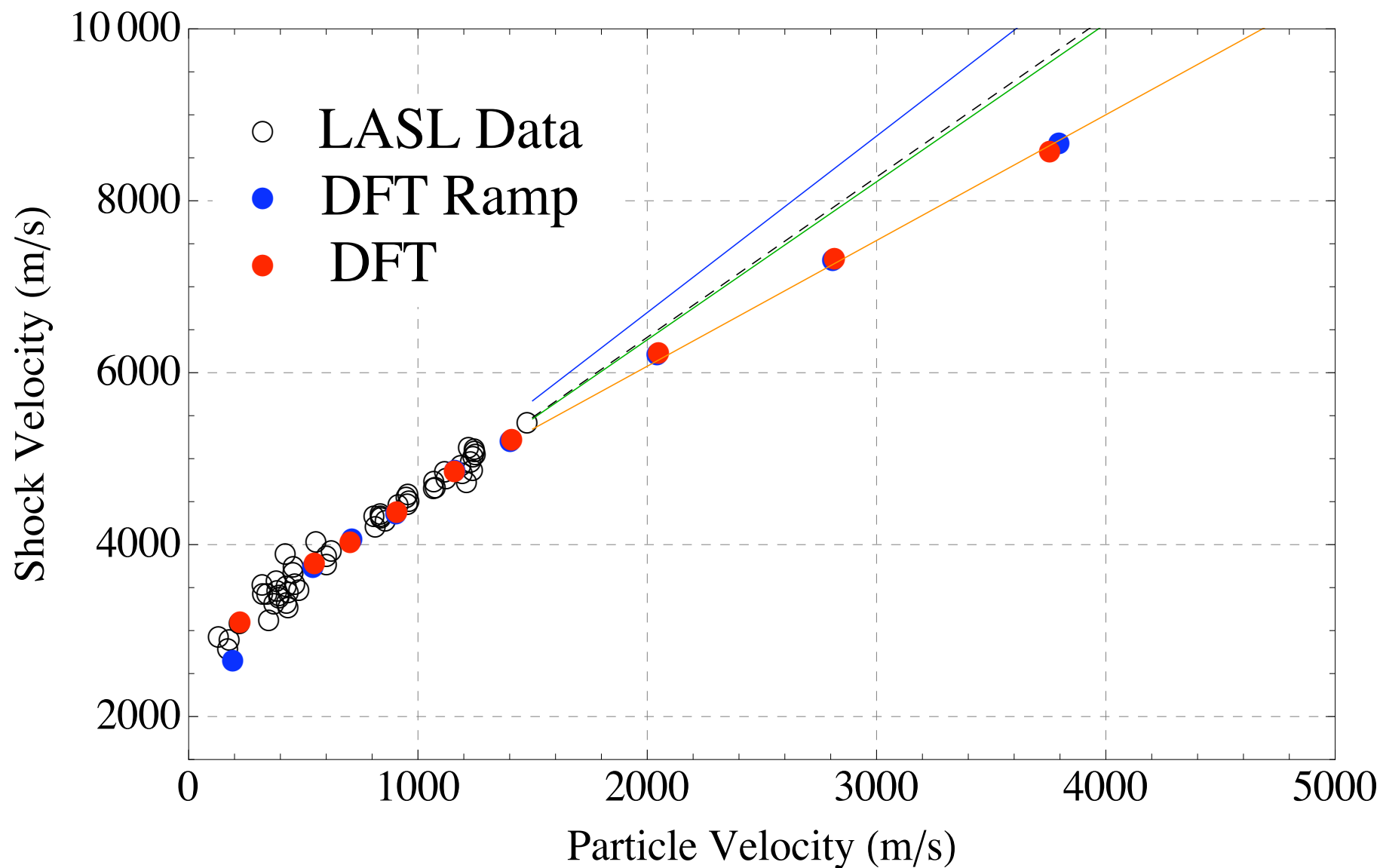
Set V, ramp T, and solve for where above is true.

Approach 2:

Set V, run several Ts, fit to P(T) and E(T) and solve.

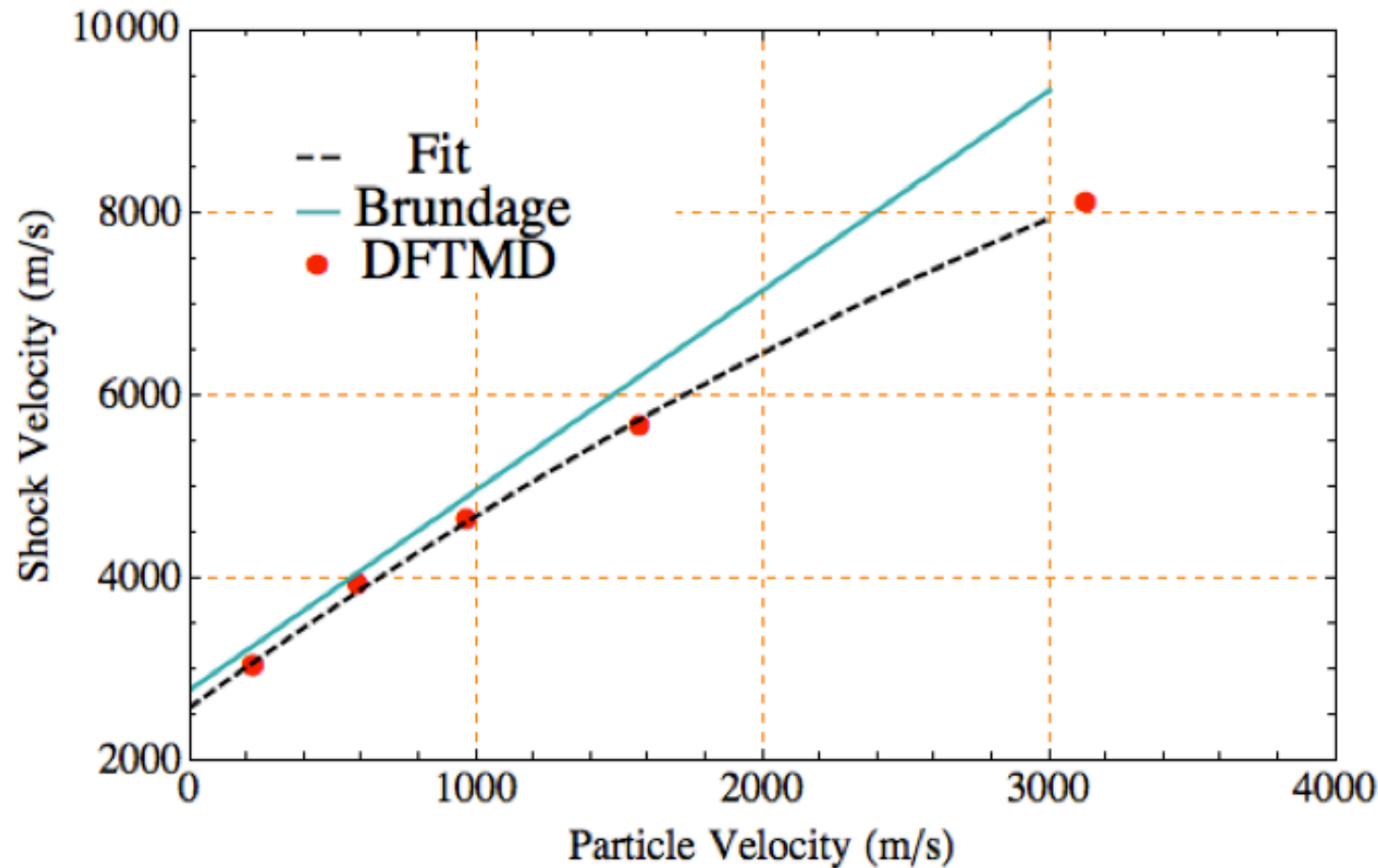
PETN

# DFT-MD calculated single crystal Hugoniot



# Epsilon CL-20

## DFT-MD calculated single crystal Hugoniot

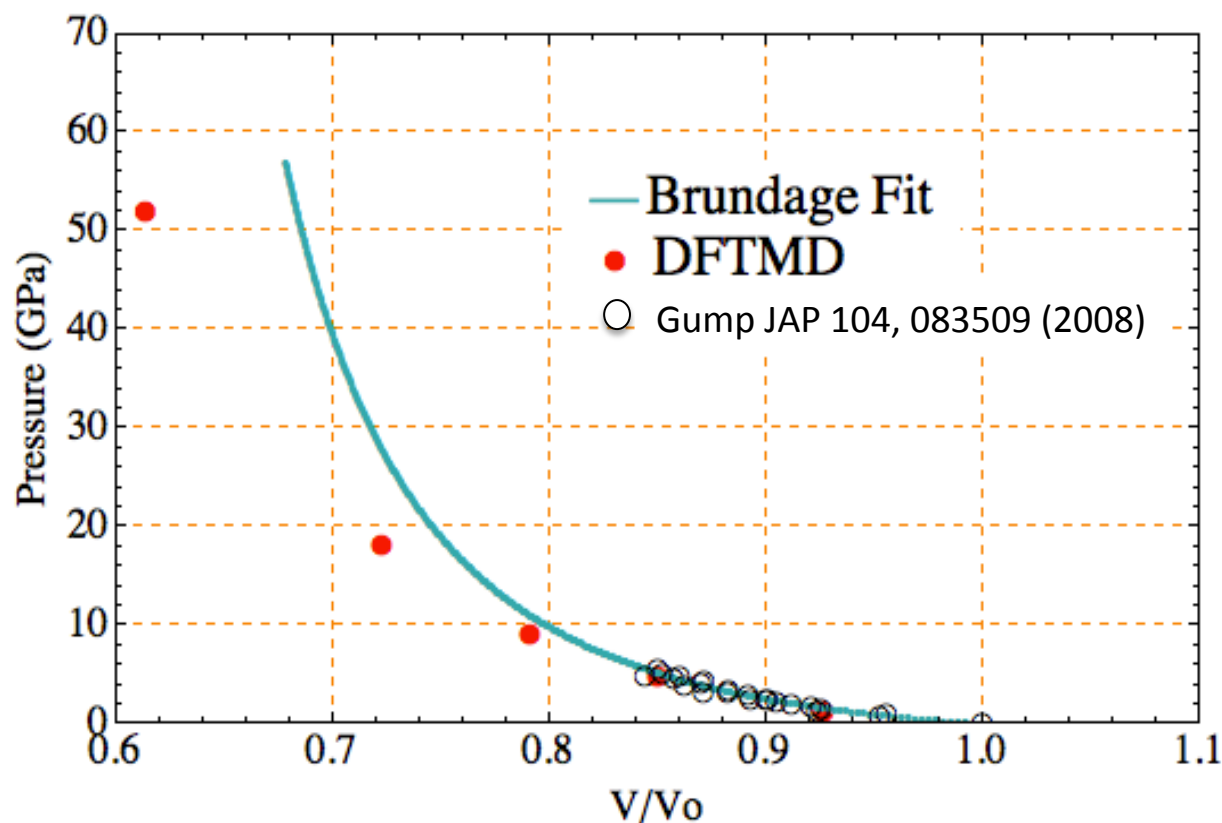


**Brundage:**  $2770 + 2.19x$  (2009 APS SCCM Proceedings)

**Second order fit to DFTMD:**  $2580.55 + 2.25161x - 0.000155591x^2$

# Epsilon CL-20

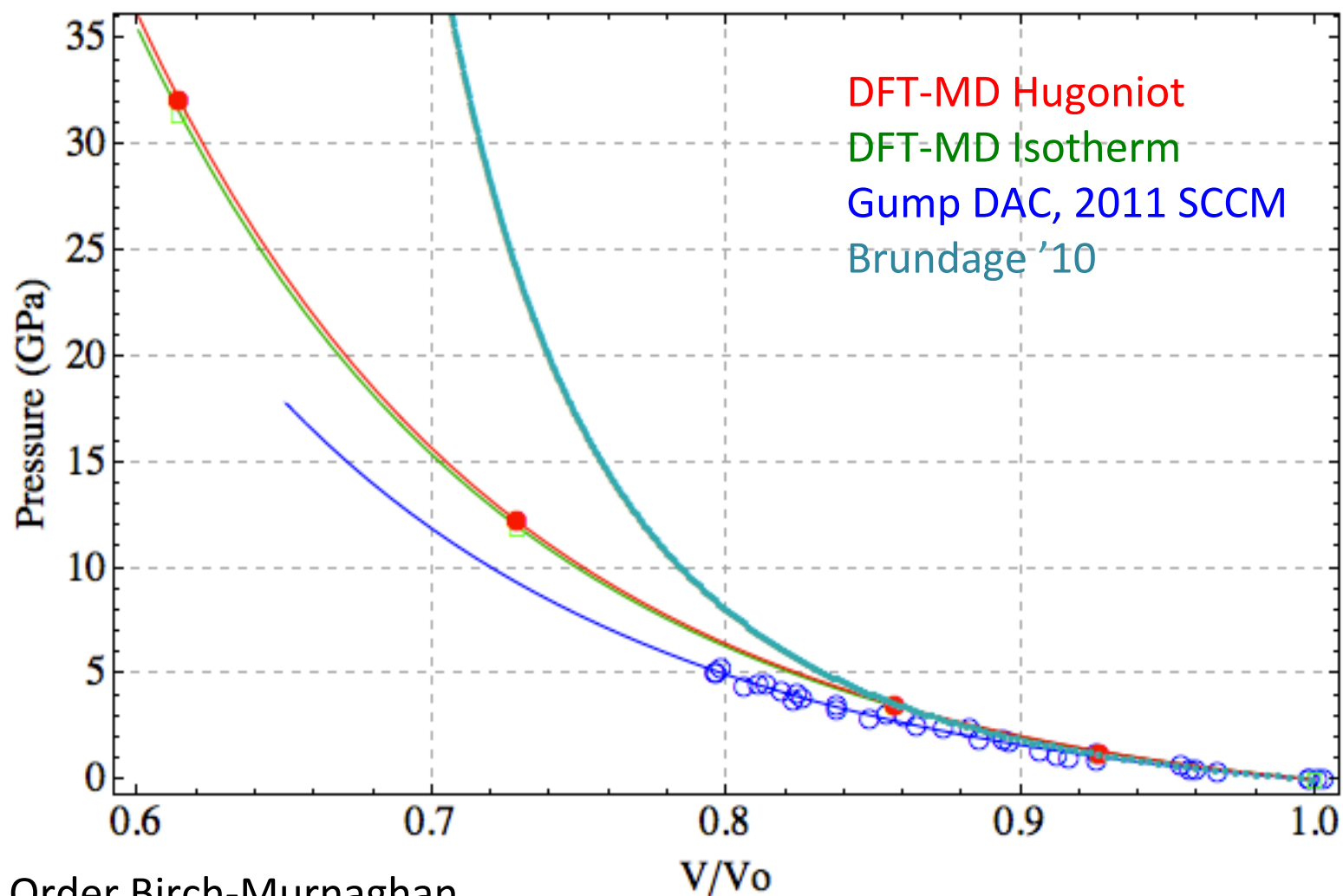
## DFT-MD calculated single crystal Hugoniot – ... and comparison with Gump's DAC experiments



**Brundage:**  $2770 + 2.19x$  (2009 APS SCCM Proceedings)



## DFT-MD calculated single crystal Hugoniot and Isotherm



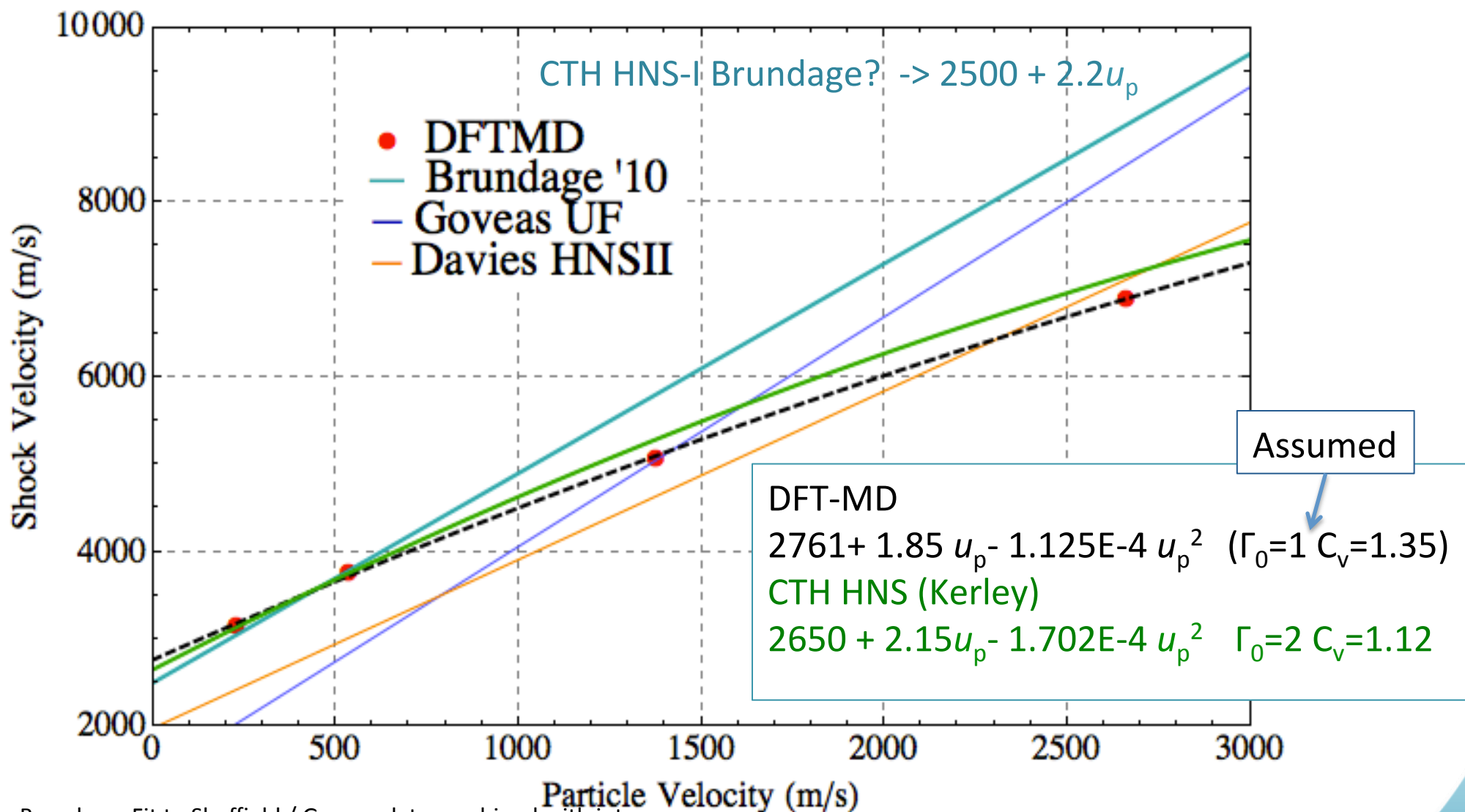
Fits: 3<sup>rd</sup> Order Birch-Murnaghan

Hugoniot →  $B_0$ : 13.7849,  $B_0'$ : 6.74949

Isotherm →  $B_0$ : 13.4739,  $B_0'$ : 6.77552

Gump DAC →  $B_0$ : 11.217,  $B_0'$ : 6.2174

# DFT-MD calculated single crystal Hugoniot



Brundage: Fit to Sheffield / Goveas data combined with inter-granular stress measurements (2010 IDS).

Goveas/Davies: fits to 91% TMD pressings APS SCCM 2005

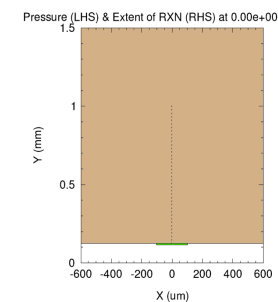
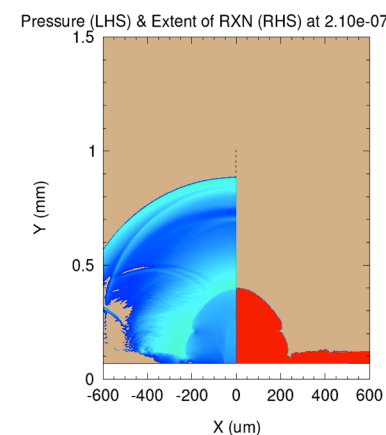
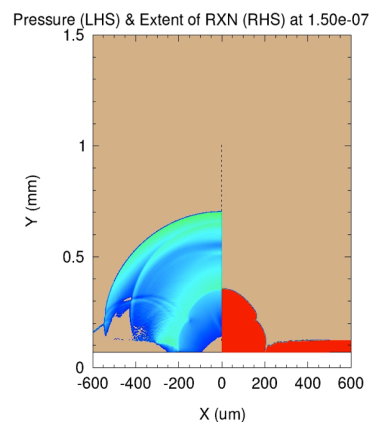
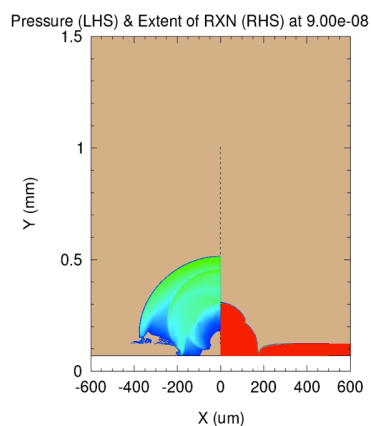
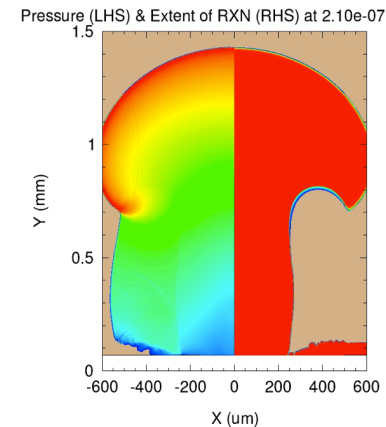
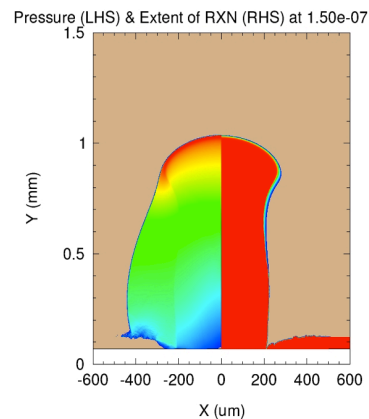
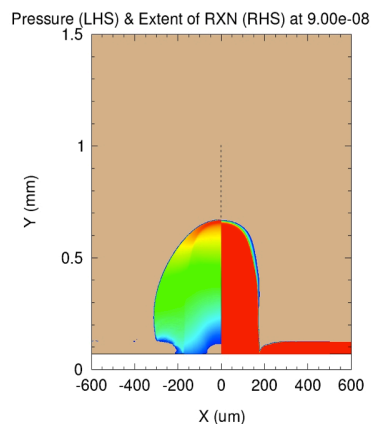
Experimental volume from Gerard and Hardy, Acta Cryst. C4 (1998) 1283-1287. Monoclinic P21/c, A=22.326, B=5.5706, C=14.667,  $\beta=110.04^\circ$

We can and will calculate  $C_v$  and  $\Gamma$

# Does it matter?

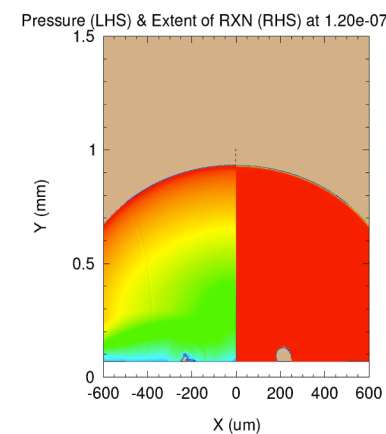
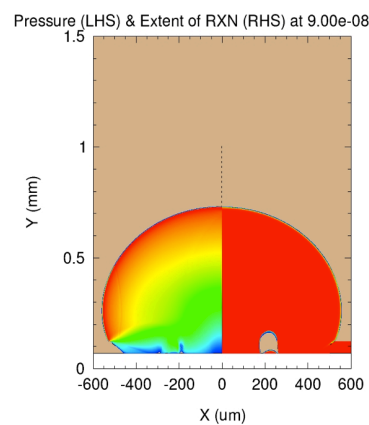
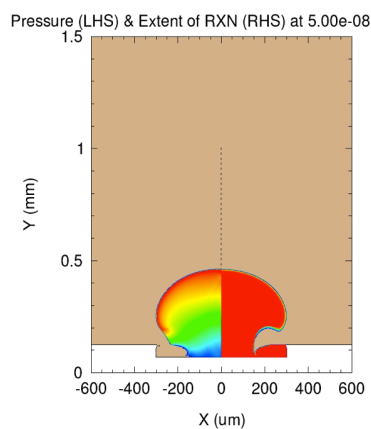
HNS-I  
(CTH ?)

$$\Gamma_0=1.0, C_v=1.35E+11$$



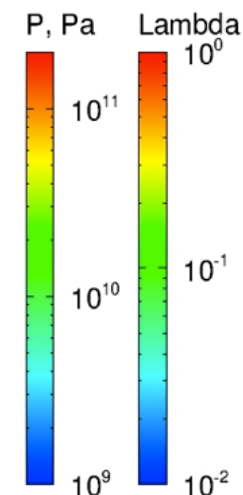
DFT-MD  
(p-alpha)

$$\Gamma_0=1.0, C_v=1.35E+11$$



HNS  
(Kerley)

$$\Gamma_0=2.0, C_v=1.12E+11$$



# Kinetic energy functionals

$$\left( -\frac{\hbar^2}{2m} \nabla^2 + v_{eff}(\mathbf{r}) \right) \psi_\nu(\mathbf{r}) = \epsilon_\nu \psi_\nu(\mathbf{r}) \quad \nu = 1, 2, \dots, N$$

$$n(\mathbf{r}) = \sum_{\nu=1}^N |\psi_\nu(\mathbf{r})|^2$$

$$v_{eff}(\mathbf{r}) = v(\mathbf{r}) + \int \frac{n(\mathbf{r}')}{|\mathbf{r} - \mathbf{r}'|} d\mathbf{r}' + \frac{\delta E_{xc}[n(\mathbf{r})]}{\delta n(\mathbf{r})}$$



$$E[n] = T_s[n] + E_{ext}[n] + E_{hartree}[n] + E_{xc}[n]$$

Minimize wrt density:  $\delta E / \delta n = 0$

# Kinetic energy functionals

Calculate the kinetic energy density  $\tau = T_s/V$  for a uniform electron gas.  
 Calculate the electron density  $n$  for a uniform electron gas.

Express  $T_s$  as a functional of the density  $n$ ,  $T_s[n]$ .

This is the Thomas-Fermi approximation for the kinetic energy.

$$\left. \begin{aligned} \tau_{\text{UEG}} &= k_F^5/5/\pi^2 \\ n_{\text{UEG}} &= k_F^3/3/\pi^2 \end{aligned} \right\} \longrightarrow \tau_{\text{TF}} = 3/5 (3\pi^2)^{2/3} n^{5/3}$$

This is corresponding to LDA for exchange-correlation functionals

# Kinetic energy functional for surface system

Calculate the kinetic energy density for a surface system

Calculate the electron density for a surface system

Express  $T_s$  as a functional of the density  $n$

This is a surface approximation for the kinetic energy.

We can easily calculate  $\tau$  for the Airy gas. We have  $n$  for an Airy gas.

We need to express  $\tau$  as a function of  $n$  and its derivatives.

Possibly we need to use an interpolation index to interpolate between TF and Airy. Need to remember to use same definition for all subsystems.

Vitos et al have made a parameterization: PRA **61**, 052511 (2000).

This is corresponding to LAA and LAG for exchange functionals.



# Kinetic energy functional for confined systems

Calculate the kinetic energy density for a confined system  
Calculate the electron density for a confined system

Express  $T_s$  as a functional of the density  $n$

This is a confined system approximation for the kinetic energy.

We can easily calculate  $\tau$  for the Harmonic Oscillator (HO) gas. We have  $n$  for a HO gas.

We need to express  $\tau$  as a function of  $n$  and its derivatives.

Possibly we need to use an interpolation index to interpolate between HO, TF, and Airy. Need to remember to use same definition for all subsystems.

# Temperature

There is no additional problem to add temperature to this scheme. Just one more parameter to account for in the parameterization procedure.

# VASP PAW potentials: Standard (old) Kr

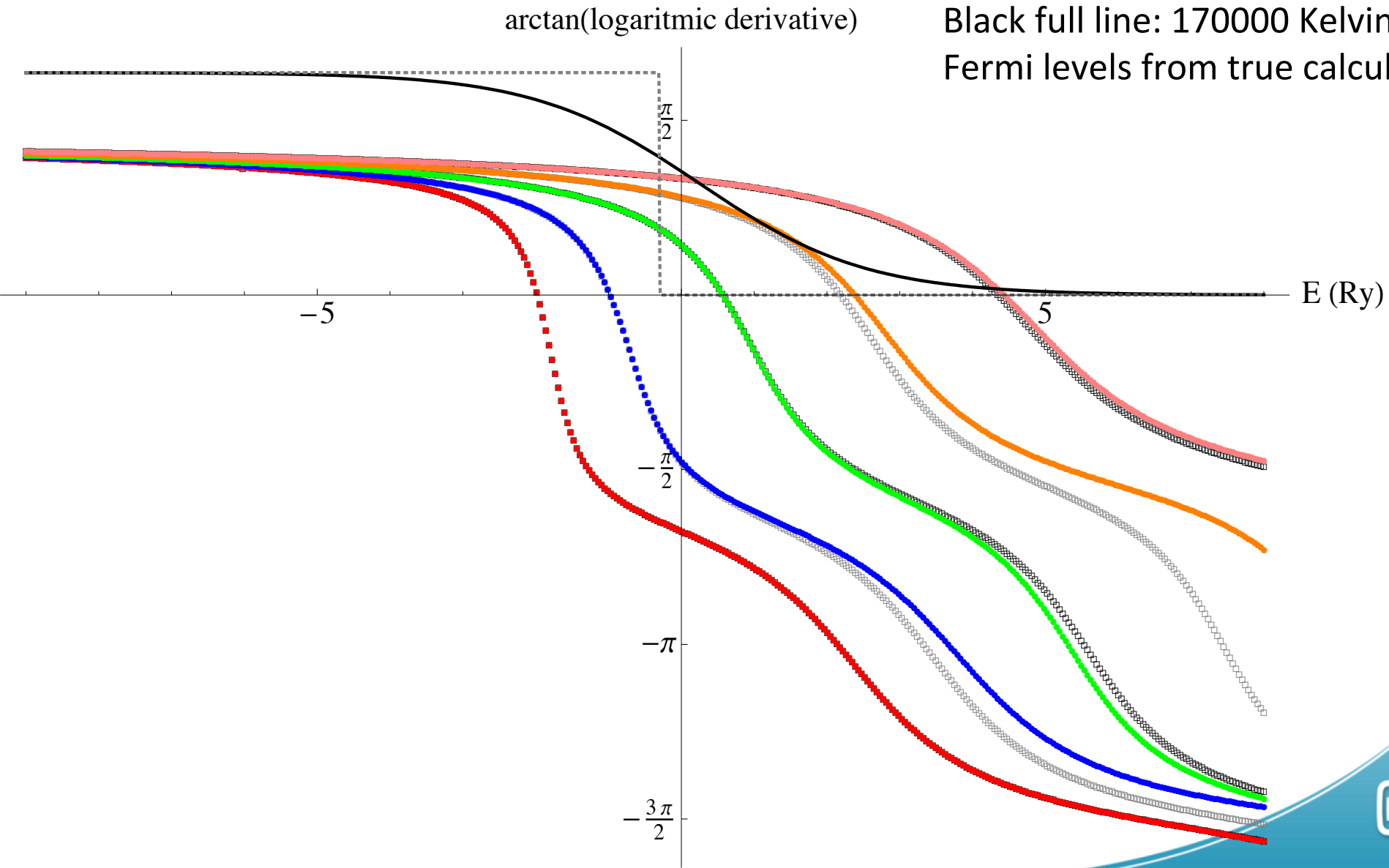
PAW Kr 07Sep2000AEM

RWIGS = 2.50 bohr

$\ell$ =s(red), p(blue), d(green, local), f(orange, local), 4(pink, local).

Gray dotted line: 300 Kelvin  
Black full line: 170000 Kelvin  
Fermi levels from true calculations.

Ann E Mattsson



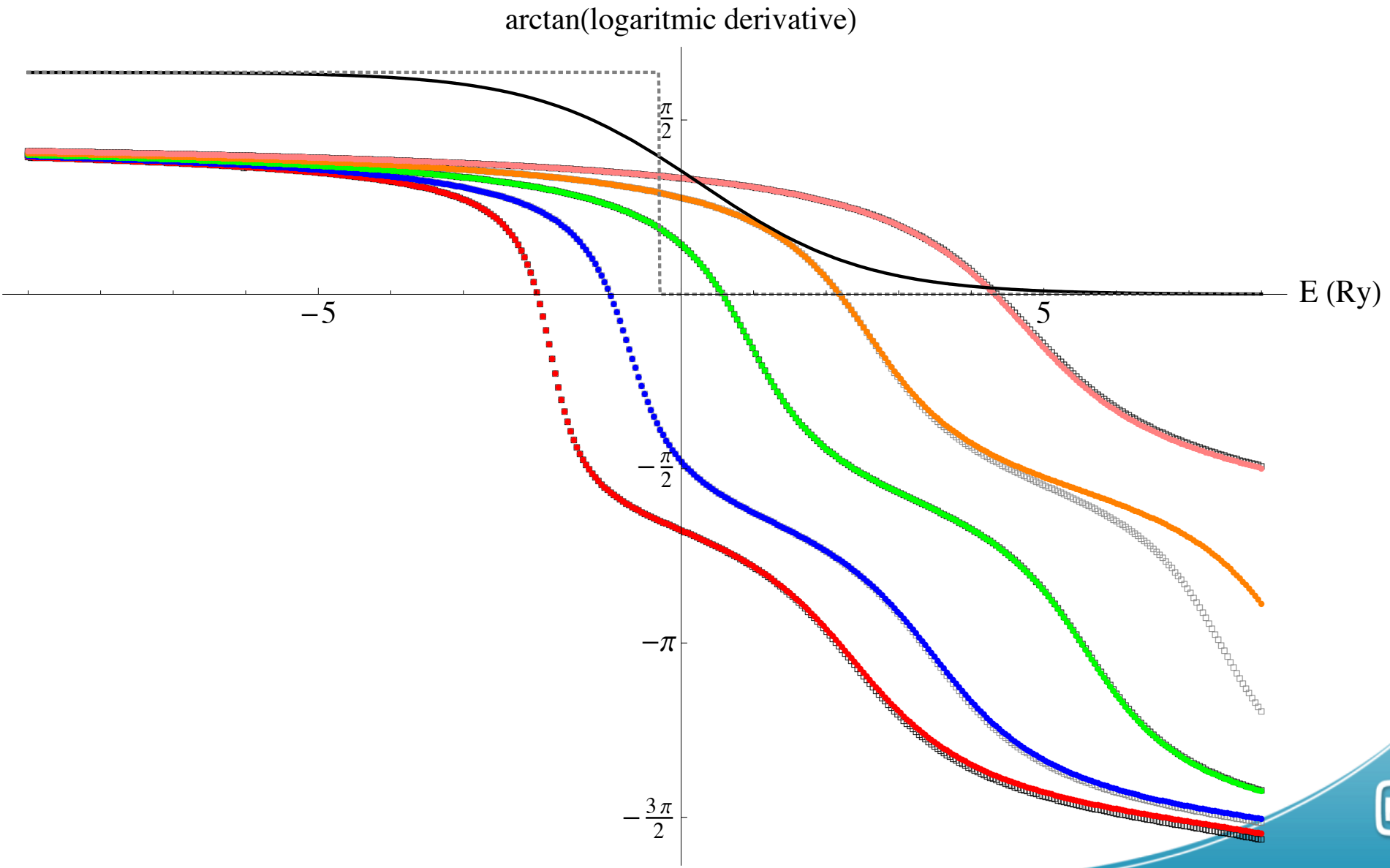
# PAW potentials: Still 8 electrons

PAW Kr 27Jan2010AEM

RWIGS = 2.50 bohr

$\ell$ =s(red), p(blue), d(green), f(orange, local), 4(pink, local).

Ann E Mattsson



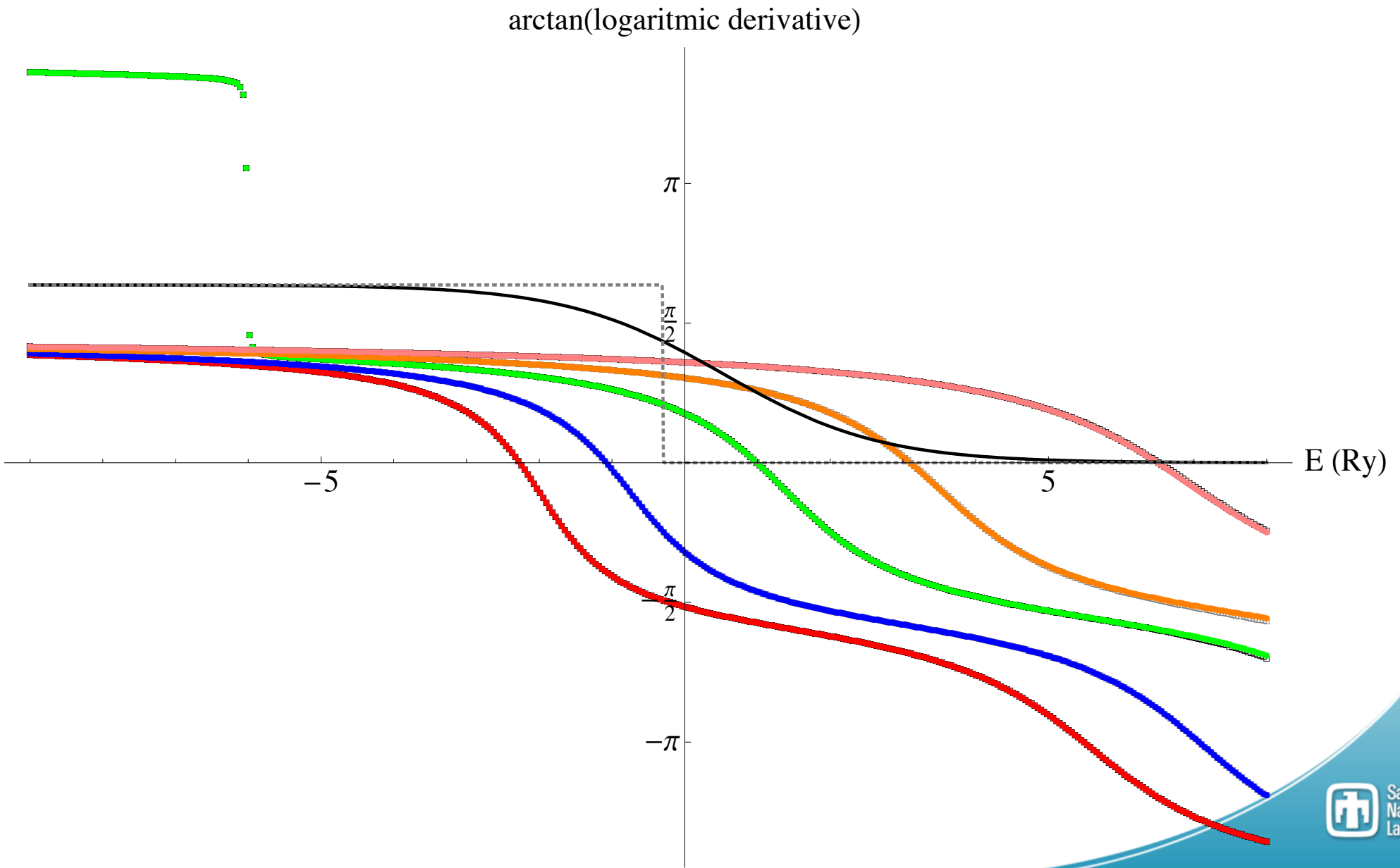
# PAW potentials: Now 18 electrons

PAW Kr18 v3 Feb2011AEM

RWIGS = 2.00 bohr

$\ell$ =s(red), p(blue), d(green), f(orange, local), 4(pink, local).

Ann E Mattsson



# Summary

- The warm dense matter region poses a particular challenge with its multitude of phases and competing physical processes.
- Experiments are of limited usefulness due to limitations in accessible parameter space. Accurate computational tools would be valuable complements.
- Even the largest and fastest computer will give us useless results if the equations implemented are the wrong ones or if the computational approach has limited accuracy.
- Density Functional Theory has the potential to provide us with the generally accurate and fast computational tool we need.
- We have implementing the DFT-Dirac equations needed to describe actinide materials.
- We are working on a general functional that would allow us to incorporate the confinement physics of the HO model system in a self-consistent way.
- The subsystem functionals scheme is a promising approach also for kinetic energy functionals.



# Thank you for your attention.

E-mail: [aematts@sandia.gov](mailto:aematts@sandia.gov)

Website with publications: <http://www.cs.sandia.gov/~aematts/>